

LONG-TERM DYNAMIC RESPONSE OF HAGIA SOPHIA IN ISTANBUL TO
EARTHQUAKES AND ATMOSPHERIC CONDITIONS

by

Emrullah Dar

B.S., Civil Engineering, Istanbul University, 2010

Submitted to the Kandilli Observatory and Earthquake

Research Institute in partial fulfillment of

the requirements for the degree of

Master of Science

Graduate Program in Earthquake Engineering

Boğaziçi University

2015

ACKNOWLEDGEMENTS

I would like to express my deepest gratitude to my advisor Prof. Eser aktı for her full support, expert guidance, understanding and encouragement throughout my study and research. In addition, I express my appreciation to Prof. Erdal Őafak, Assoc. Prof. Őmit Dikmen and Assoc. Prof. Ufuk Hancılar for their help with academic research and for computational support.

I would also like to thank Ahmet Korkmaz, Ayten Korkmaz and Göken Turan Kara for working devotedly on the collection of data. I am so glad to work with helpful and gracious friends. I wish to express my great thanks to Saed Moghimi for his patience and guidance on my thesis. Also, I want to thank Esra Zengin and Dr. Őzden Ateő Saygılı for their helpfulness. I also want to express my special thanks to my roommate Yavuz Őz for his supports and advices.

Finally, I would like to thank my mother, father and sisters for their unconditional love and support during this study and in all my experience.

ABSTRACT

LONG-TERM DYNAMIC RESPONSE OF HAGIA SOPHIA IN ISTANBUL TO EARTHQUAKES AND ATMOSPHERIC CONDITIONS

The effects of atmospheric factors on structural behavior have gained more importance due to climate change as result of global warming in recent years. In this thesis, the effects of ground motions and atmospheric variations on the modal parameters of Hagia Sophia in Istanbul, which is one of the most prominent structures created in the history and is in the UNESCO world heritage list, are examined.

Firstly, the frequency variation of Hagia Sophia due to atmospheric conditions such as temperature, wind speed, humidity and precipitation has been assessed. For this purpose, acceleration records are divided into half-hour segments and the Fourier amplitude spectra of each segment are calculated using short-time Fourier transform. In this way, an annual frequency variation of the structure is achieved by combination of frequency values obtained from these spectra. Afterwards, the frequency variation of Hagia Sophia is compared with the variation of atmospheric conditions and the results are assessed individually.

Secondly, the dynamic behavior of the Hagia Sophia during different earthquakes is analyzed. The modal parameters and mode shapes of the structure are determined. The decrease associated with the first two modal frequencies of the structure during each earthquake is calculated. Finally, the effect of maximum acceleration and duration of strong ground motion on modal frequencies of the structure is investigated.

ÖZET

AYASOFYA’NIN DEPREMLER VE ATMOSFER KOŞULLARI ALTINDAKİ DİNAMİK DAVRANIŞ ÖZELLİKLERİ

Son yıllarda, küresel ısınmaya bağlı iklim değışikliklerinin etkilerinin artması ile birlikte, atmosfer koşullarının yapılar üzerindeki etkileri önem kazanmıştır. Bu tezde, değışen atmosferik koşulların ve depremlerin sanat tarihinin en önemli eserlerinden biri olan ve UNESCO dünya kültür mirası listesinde bulunan Ayasofya’nın modal parametreleri üzerindeki etkileri incelenmiştir.

İlk olarak, Ayasofya’nın sıcaklık, rüzgâr hızı, nem ve yağış miktarı gibi atmosferik faktörlere bağlı frekans değışimi gözlemlenmiştir. İvme kayıtları yarım saatlik segmentlere bölünmüş ve bu segmentlerin kısa zamanlı Fourier dönüşümü metodu yardımıyla, Fourier büyüklük spektrumları elde edilmiştir. Bu spektrumlardan elde edilen frekans değeri birleştirilerek, bir yıllık frekans değışimi elde edilmiştir. Daha sonra bu frekans değışimi tek tek atmosferik faktörler ile kıyaslanmış ve sonuçlar değerlendirilmiştir.

İkinci olarak ise, Ayasofya’nın farklı depremler etkisi altındaki dinamik davranışı incelenmiştir. Yapının modal parametreleri ve mod şekilleri her deprem için belirlenmiştir. Daha sonra, her deprem için yapının frekansındaki düşme miktarı incelenmiş ve bu düşüşün depremin ivmesi ve süresi ile ilişkisi irdelenmiştir.

TABLE OF CONTENTS

ACKNOWLEDGEMENTS.....	iii
ABSTRACT.....	iv
ÖZET.....	v
LIST OF FIGURES.....	viii
LIST OF TABLES.....	xiii
1. INTRODUCTION.....	1
1.1. Objective.....	1
1.2. Justification for the Study.....	2
1.3. Hagia Sophia.....	3
1.4. Organization of Thesis.....	4
2. LITERATURE REVIEW.....	5
2.1. Earthquake Response of Hagia Sophia.....	5
2.2. Effect of Atmospheric Conditions on Structural Modal Response.....	7
3. HAGIA SOPHIA VIBRATION MONITORING SYSTEM, DATA AND DATA PROCESSING.....	10
3.1. Hagia Sophia Structural Vibration Monitoring System.....	10
3.2. Atmospheric Data.....	12
3.3. Earthquake Data.....	13
3.4. Data Processing.....	20
4. EFFECT OF ATMOSPHERIC CONDITIONS ON MODAL FREQUENCY AND MODAL DAMPING.....	23
4.1. Temperature.....	23
4.2. Wind.....	32
4.3. Precipitation.....	35
4.4. Humidity.....	39
5. ANALYSIS OF EARTHQUAKE RESPONSE.....	43
5.1. Time Domain Properties.....	43
5.2. Frequency Domain Properties.....	49
5.3. Mode Shapes.....	53
5.4. Variation of Modal Frequencies with Vibration Amplitude and Duration.....	59
6. CONCLUSIONS.....	62

REFERENCES..... 64

LIST OF FIGURES

Figure 3.1. Hagia Sophia structural monitoring system; the isometric view is from Mainstone (2006).....	11
Figure 3.2. Locations of three-component accelerometric stations in Hagia Sophia.....	12
Figure 3.3. Location of Hagia Sophia in the historical peninsula of Istanbul.....	13
Figure 3.4. Epicenters of earthquakes recorded in Hagia Sophia.....	15
Figure 3.5. Epicenters of earthquakes in the Marmara region recorded in Hagia Sophia	15
Figure 3.6. Steps for preparation and analysis of data for long term analysis.....	22
Figure 4.1. Variation of first modal frequency at station GAL1 and temperature in year 2013 (X direction).....	24
Figure 4.2. Variation of first modal frequency at station GAL2 and temperature in year 2013 (X direction).....	25
Figure 4.3. Variation of first modal frequency at station KUB1 and temperature in year 2013 (X direction).....	25
Figure 4.4. Variation of first modal frequency at station KUB2 and temperature in year 2013 (X direction).....	26
Figure 4.5. Variation of second modal frequency at station GAL1 and temperature in year 2013 (Y direction).....	26

Figure 4.6. Variation of second modal frequency at station GAL2 and temperature in year 2013 (Y direction).....	27
Figure 4.7. Variation of second modal frequency at station KUB1 and temperature in year 2013 (Y direction).....	27
Figure 4.8. Variation of second modal frequency at station KUB2 and temperature in year 2013 (Y direction).....	28
Figure 4.9. Variation of first modal frequency at station KUB1 and temperature between 13.06.2013 and 26.06.2013 (X direction).....	28
Figure 4.10. Variation of second modal frequency at station KUB1 and temperature between 13.06.2013 and 26.06.2013 (Y direction).....	29
Figure 4.11. Variation of second modal frequency at station KUB1 and temperature during the first 15 days of February 2013 (X direction).....	29
Figure 4.12. Variation of second modal frequency at station KUB1 and temperature during the first 15 days of February 2013 (Y direction).....	30
Figure 4.13. Variation of mean damping ratio and temperature in year 2013 (X direction).....	31
Figure 4.14. Variation of mean damping ratio and temperature in year 2013 (Y direction).....	31
Figure 4.15. Variation of first modal frequency at station KUB1 and wind speed in year 2013 (in X direction).....	33
Figure 4.16. Variation of second modal frequency at station KUB1 and wind speed in year 2013 (in Y direction).....	34

Figure 4.17. Variation of first modal frequency at station KUB1 and wind speed between 04.01.2013 and 30.01.2013 (in X direction).....	34
Figure 4.18. Variation of second modal frequency at station KUB1 and wind speed between 04.01.2013 and 30.01.2013 (in Y direction).....	35
Figure 4.19. Variation of first modal frequency at station KUB1 and precipitation in year 2013 (in X direction).....	36
Figure 4.20. Variation of second modal frequency at station KUB1 and precipitation in year 2013 (in Y direction).....	37
Figure 4.21. Variation of first modal frequency at station KUB1 and precipitation between 04.01.2013 and 28.01.2013 (in X direction).....	37
Figure 4.22. Variation of frequency/temperature ratio at station KUB1 and precipitation between 10.06.2013 and 25.06.2013 (in X direction).....	38
Figure 4.23. Variation of second modal frequency at station KUB1 and precipitation between 04.01.2013 and 28.01.2013 (in Y direction).....	38
Figure 4.24. Variation of frequency/temperature ratio at station KUB1 and precipitation between 10.06.2013 and 25.06.2013 (in Y direction).....	39
Figure 4.25. Variation of first modal frequency at station KUB1 and humidity in year 2013 (in X direction).....	40
Figure 4.26. Variation of frequency/temperature ratio at station KUB1 and humidity between 10.06.2013 and 25.06.2013 (in X direction).....	41
Figure 4.27. Variation of second modal frequency at station KUB1 and humidity in year 2013 (in Y direction).....	41

Figure 4.28. Variation of frequency/temperature ratio at station KUB1 and humidity between 10.06.2013 and 25.06.2013 (in Y direction).....	42
Figure 5.1. Peak horizontal (X) accelerations recorded at Hagia Sophia stations.....	45
Figure 5.2. Peak horizontal (Y) accelerations recorded at Hagia Sophia stations.....	45
Figure 5.3. Peak vertical accelerations recorded at Hagia Sophia stations.....	46
Figure 5.4. Peak horizontal (X) velocities at Hagia Sophia stations.....	46
Figure 5.5. Peak horizontal (Y) velocities at Hagia Sophia stations.....	47
Figure 5.6. Peak vertical velocities at Hagia Sophia stations.....	47
Figure 5.7. Peak horizontal (X) displacements at Hagia Sophia stations.....	48
Figure 5.8. Peak horizontal (Y) displacements at Hagia Sophia stations.....	48
Figure 5.9. Peak vertical displacements at Hagia Sophia stations.....	49
Figure 5.10. Identified first modal frequencies at Hagia Sophia stations during fifteen largest earthquakes that produced largest vibration amplitudes (X direction).....	50
Figure 5.11. Identified second modal frequencies at Hagia Sophia stations during fifteen largest earthquakes that produced largest vibration amplitudes (Y direction).....	51
Figure 5.12. Fourier amplitude spectrum of station KUB2 during M6.5 Aegean Sea Earthquake in X direction.....	52

Figure 5.13. Fourier amplitude spectrum of station KUB2 during M6.5 Aegean Sea Earthquake in Y direction.....	52
Figure 5.14. Particle motions corresponding to first modal frequency at Hagia Sophia stations during 6.5 Aegean Sea Earthquake.....	55
Figure 5.15. Particle motions corresponding to second modal frequency at Hagia Sophia stations during 6.5 Aegean Sea Earthquake.....	56
Figure 5.16. Particle motions corresponding to first modal frequency at stations GAL4 and KUB4 during three earthquakes.....	57
Figure 5.17. Particle motions corresponding to second modal frequency at stations GAL4 and KUB4 during three earthquakes.....	58
Figure 5.18. Drop in first and second modal frequencies with respect duration.....	60
Figure 5.19. Drop in first and second modal frequencies with respect to peak acceleration at the ground level of Hagia Sophia.....	61

LIST OF TABLES

Table 3.1. Earthquakes recorded in the time interval between 2008 and 2012 in Hagia Sophia.....	16
Table 3.2. Earthquakes recorded in 2013 in Hagia Sophia.....	17
Table 3.3. Earthquakes recorded in first six months of 2014 in Hagia Sophia.....	18
Table 3.4. Earthquakes recorded in last six months of 2014 in Hagia Sophia.....	19

1. INTRODUCTION

1.1. Objective

The main objective of this study is to investigate long-term dynamic response of Hagia Sophia in Istanbul to earthquakes and atmospheric conditions. It is aimed to display the variation in time and frequency domain dynamic response parameters of Hagia Sophia due to external sources and to identify behavioral patterns that can be associated with changes in the atmospheric conditions. At the same time the vibration levels throughout the structure are studied to identify anything that stand out and can be interpreted as possible local or general structural problems.

Atmospheric conditions affect modal vibration frequencies and damping coefficients of a building. Daily and seasonal variations in the temperature for example, induce continuous cyclic variation in the dynamic response. In this thesis the effect of atmospheric phenomena such as temperature, wind speed, precipitation and humidity on structural vibration properties of Hagia Sophia is investigated. It is aimed at exploring the degree of each atmospheric effect on the response parameters of the building.

It is well known that not only excessive earthquake vibrations, but also low and moderate level excitations effect buildings as well. Using acceleration data recorded during low to moderate magnitude earthquakes since 2008 in Hagia Sophia, we aim to explore the dynamic properties of the building. Structural parts and elements that respond differently than the overall structure are detected. Additionally, it is aimed to observe the amount of frequency decrease of the structure with respect to maximum acceleration and significant duration of strong ground motion.

1.2. Justification for the Study

Many studies have been conducted on the dynamic behavior of Hagia Sophia up to now. Different groups studied earthquake response of Hagia Sophia using numerical modeling and/or actual earthquake records in order to investigate its vibration characteristics, to understand the mechanisms involved in past damages, to assess its vulnerability to future large earthquakes and to propose alternatives for strengthening. However, there is no study yet in the literature investigating the effect of atmospheric conditions on the dynamic behavior of Hagia Sophia. In fact this is a relatively new issue. There are only a handful of studies in the literature concerning the frequency variation of buildings due to atmospheric changes. Present studies show that atmospheric conditions do not affect the structures in the same way due to differences in construction materials and structural systems. Therefore, these effects need to be monitored and analyzed across different structural systems and construction materials.

The earthquake monitoring system in Hagia Sophia installed in 1991 was trigger-based. It was replaced in 2008 by a new system that records the response of the structure continuously and transmits the data to the data center at the Department of Earthquake Engineering in real time. The availability of continuous data enables the study of long-term effects such as atmospheric conditions on dynamic response parameters. The new system detects and records not only events that take place in relatively close locations, but also earthquakes that take place at far more distant locations such as the 2011 Van Earthquake. As such, a significant number of earthquake recordings are now available for analysis of the earthquake behavior of Hagia Sophia, providing an excellent opportunity for further investigation of the issues raised by Durukal *et al.* (2003) regarding the frequency and duration dependence of modal frequencies of Hagia Sophia and its vibration characteristics in time domain.

1.3. Hagia Sophia

The Hagia Sophia in Istanbul is artistically, historically and culturally unprecedented with its grandness, architecture and spirituality. It is included in the world heritage list of UNESCO in 1985. The planners of Hagia Sophia, Isidore of Miletus and Anthemius of Tralles designed it as a combination of a centralized structure and a longitudinal basilica. The construction period (532 – 537) lasted slightly over 5 years, which is a relatively short period of time given its size, structural complexity and the use of masonry as the construction material. The longitudinal length of the structure is 100 m, while its width is 69.5 m. The height between the central dome and the ground level is 55.60 m. The diameter of the dome is 31.87 m in the north - south direction and 30.86 m in the east - west direction. After the conquest of Istanbul by Ottoman Empire in 1453, Hagia Sophia was converted into a mosque. The structure underwent a major restoration scheme directed by Architect Sinan in the 16th century. In the republican era Hagia Sophia was converted to a museum in 1935. It serves to this day as a museum attracting visitors from all over the world as a cultural heritage building.

Hagia Sophia experienced many earthquakes in its history resulting in damages and partial collapses. The first destructive damage occurred on the eastern side of the dome in 553 during an earthquake. As a consequence, the main dome was rebuilt this time six meters higher than the original dome (Müller-Wiener, 2007). The second severe earthquake occurred in 989 and caused damage in the west main arch and collapse of the adjacent parts of the main dome. Then a wider and thicker arch was rebuilt (Van Nice, 1963). In 1349, the east main arch and the adjacent parts of the dome collapsed for the last time and rebuilt (Mainstone *et al.*, 2006). The building never collapsed as a whole.

Earthquakes damaging Hagia Sophia originate from the segments of the North Anatolian Fault Zone in the Marmara Sea, 20 km away from the south of the building at closest distance. This part of the North Anatolian Fault zone is inactive at present and has been classified as a "seismic gap" (Barka *et al.*, 1989). Due to numerous earthquakes, Hagia Sophia survived in its long history, as a consequence of its construction material (masonry), as a result of several repair and restoration schemes of varying quality carried out through

centuries, the structure has large deformations in its structural bearing elements. From earthquake engineering perspective, the dynamic behavior of the Hagia Sophia and its vulnerability to earthquakes are of academic and professional concerns.

1.4. Organization of Thesis

This thesis includes six chapters. Following this introductory part, which is Chapter 1, Chapter 2 presents the literature review. Chapter 2 is divided into two parts, where studies investigating earthquake behavior of Hagia Sophia and the effect of atmospheric conditions on structural modal response are summarized. Chapter 3 describes the earthquake monitoring system in Hagia Sophia, the atmospheric and earthquake data that was used and the particulars employed in data processing. The investigation of the effects of atmospheric conditions on modal frequency and modal damping is presented in Chapter 4. Chapter 5 presents the analysis of earthquakes recorded between 2008 and 2014 and investigates the earthquake response of Hagia Sophia. Finally, Chapter 6 summarizes and concludes the thesis.

2. LITERATURE REVIEW

2.1. Earthquake Response of Hagia Sophia

A series of studies has been conducted trying to assess Hagia Sophia's earthquake behavior by making use of vibration data. In this section some of these studies are summarized. One of the first studies was “*A Study on Structural Identification and Seismic Vulnerability Assessment of Aya Sophia*” (Çaktı, 1992). In this study, the dynamic behavior of Hagia Sophia was investigated. The modal frequencies and mode shapes of the structure were obtained from ambient vibration surveys and on the basis of the finite element model of the structure. This study paved the way for new studies to examine the dynamic behavior of Hagia Sophia.

Structural Analysis of Hagia Sophia: A Historical Perspective by Mark et al. (1993): Within the study, a different perspective was proposed to specify earthquake response of Hagia Sophia. The study discussed possible design antecedents and aspects of the structure's constructional history as well as the criterion of numerical designs of the primitive structure that explain both short- and long-term, linear and nonlinear material behavior.

The Mother of All Churches: A Static and Dynamic Structural Analysis of Hagia Sophia by Davidson (1993): In this study, Davidson applied a series of finite element analyses in order to determine the static and dynamic behaviors of Hagia Sophia. The models are consists of static linear elastic model, dynamic linear elastic model, static nonlinear model, dynamic nonlinear model and time history analysis.

Strong-motion Instrumentation of Aya Sofya and the Analysis of Response to an Earthquake of 4.8 Magnitude by Erdik et al. (1993): The aim of the study was to compare modal vibration frequencies and the mode shapes obtained by empirical transfer functions with analytical finite element studies. In this study, Karacabey Earthquake that was recorded in 1992 with $M_b=4.8$ were used to perform this comparison.

Structural Characteristics of the Dome of Hagia Sophia from Measurement of Micro Tremor by Aoki et al. (1993): The objective of the study was to clarify the characteristics of the dome of Hagia Sophia as a whole. Researchers determined the frequency variation of structural elements of the structure using microtremors. In addition, the south-west minaret of Hagia Sophia was also analyzed.

Dynamic Analysis and Earthquake Response of Hagia Sophia by Çakmak et al. (1993): In this study, the dynamic behavior of Hagia Sophia was analyzed; modal parameters and mode shapes of the structure were determined. Moreover, it was proposed that the animation of actual measured responses of the structure clarify the mode shapes and eigen values frequencies.

Interdisciplinary Study of Dynamic Behavior and Earthquake Response of Hagia Sophia by Çakmak et al. (1994): In this study, Hagia Sophia was analyzed in many aspects. A numerical model was used to predict the measured responses. On the other hand, the improvements obtained by incorporating soil-structure interaction were presented. The materials constituting the mortar were examined in detail benefiting from a number of preliminary microstructural, mineralogical, and chemical experiments to support the selection of actual mechanical properties. The foundations of the main columns and soil surrounding them were studied through preliminary tomography tests to corroborate the modeling of soil-structure interaction.

Principle of Structural Restoration for Hagia Sophia Dome by Aoki et al. (1997): The authors offered some important suggestions for the renovation of the dome of Hagia Sophia. They examined the modal parameters and estimated the young's modulus of materials of the structure. Finally, finite element elasto-plastic analysis was performed and suitable restoration suggestions were offered to address structural weaknesses.

Dynamic Response of Two Historical Monuments in Istanbul Deduced from the Recordings of Kocaeli and Düzce Earthquakes by Durukal et al. (2003): The aim of the

study was to observe the effect of 17 August 1999, Kocaeli (Mw 7.4) and 12 November 1999, Düzce, Turkey (Mw 7.2) earthquakes on Hagia Sophia and Süleymaniye Mosque. The variation of frequency with acceleration and duration was examined. Local structural problems were investigated in both structures. The effect of ground motion amplitude on frequency drop of the structures was discussed. Modal shapes and first-order estimates of modal damping of the two historical structures were also specified.

Tools and Techniques for Real-Time Modal Identification by Kaya et al. (2009): This study proposed a software package that identifies the real-time modal properties of structures. The software was tested on Hagia Sophia data for a two year duration. The software enables to control various algorithm schemes to identify modal properties, as well as options to plot their time variations and animations.

Re-evaluation of Earthquake Performance and Strengthening Alternatives of Hagia Sophia by Kırlangıç et al. (2009): Within this study, strengthening strategies for Hagia Sophia was proposed. For this purpose, a finite element model of the structure was used and deformations and stress distributions were determined. As a result of these analyses, two main strengthening strategies were investigated for their effectiveness. The first method was retrofitting the main arches with posttensioned bars and the second one was wrapping the structural elements with fiber-reinforced polymers.

Structural Behavior of Hagia Sophia under Dynamic Loads by Almac et al. (2014): This paper presented the preliminary results carried out using detailed finite elements models of Hagia Sophia. As a result of dynamic analysis, the east and west main arches were reiterated as the most vulnerable areas of the structure, together with adjacent portions of semi domes and the central dome.

2.2. Effect of Atmospheric Conditions on Structural Modal Response

Research in recent years shows that atmospheric conditions have a significant effect on the modal response of structures. Due to the fact that the effect of atmospheric conditions

on structural modal response is a new research topic, there are only a few studies on this subject in the literature. Studies show that the variation of temperature in particular has a much important role on structures than it was thought before, which has not been explained completely yet. The prominent studies on this issue are presented in this section.

Modern Digital Seismology - Instrumentation and Small Amplitude Studies in the Engineering World by Clinton (2004): Clinton analyzed 9th floor of Millikan Library in order to observe the response of the building to ambient weather, forced vibrations and small earthquakes that occurred during its lifetime. This study proved that there is a direct relationship between structural vibration and atmospheric conditions.

Dynamic Monitoring of a Stadium Suspension Roof: Wind and Temperature Influence on Modal Parameters and Structural Response by Martins et al. (2013): This paper clarifies the temperature and wind effect on the Braga Stadium suspension in terms of frequency and damping variation. With the purpose of obtaining a characterization of the wind action and temperature action, the vibration of the structure is monitored over a period of eight months. It is expressed that temperature increase leads to a decrease on the elasticity modulus of the concrete and increase on the natural vibration of structures. Another important conclusion is that for all examined modes, the change of the damping ratio is more associated with the variation of mean wind speed rather than mean temperature.

Frequency and Damping Wandering in Existing Buildings Using the Random Decrement Technique by Gueguen et al. (2014): This study is focused on the long-term variation of frequency and damping in several buildings, using the random decrement technique. This technique provides a rapid, robust and accurate long-term analysis and improves the reliability of frequency and damping measurements for structural health monitoring. This technique finds out particularly proper information in observing how far the variation of modal parameters can be related to the variation of physical properties. This study highlights the reversible variations of the structure's dynamic parameters, correlated with external forces, such as temperature and exposure to the sun. The results show that there

is a positive correlation between frequency and temperature and this effect is changing according to the time interval considered: daily or seasonal.

Evaluation of the Environmental Effects on a Medium Rise Building Boroschek et al. (2014): This study presents the variation of the dynamic parameters due to environmental effects of the Central Tower at the Faculty of Physical and Mathematical Science of the University of Chile. The installed network takes into consideration the environmental conditions, such as wind speed and direction, temperature, radiation, rainfall, ambient and soil humidity. The results of the study show that frequency variation rate due to temperature is about 4% and it also depends on the rain and the surrounding soil humidity around the ratio of 6%. The effect of strong ground motion on the frequency variation is also observed. Earthquake damage during the 2010 Mw=8.8 Earthquake was clearly identified from ambient vibration and earthquake records. Variations due to this damage are in the range of 15 to 20% for predominant natural frequencies.

3. HAGIA SOPHIA VIBRATION MONITORING SYSTEM, DATA AND DATA PROCESSING

3.1. Hagia Sophia Structural Vibration Monitoring System

Structural health monitoring systems facilitate the estimation of modal parameters of structures under the influence of environmental factors. They assess the indications of operational incidents, anomalies, and/or deterioration or damage that may affect operation, serviceability, safety and reliability (Aktan, 2000). The layout of sensors used in structural monitoring; their type, number and location are essential for an efficient observation of structural response parameters.

The vibration monitoring system in Hagia Sophia was established in August 1991. After the first installation, in addition to small magnitude events, important earthquakes such as the Kocaeli Earthquake on 17 August 1999 and the Düzce Earthquake on 12 November 1999 were recorded by the sensors of the system (Durukal *et al.*, 2003; Erdik *et al.*, 1993; Çakmak *et al.*, 1993; Çaktı, 1992). In November 2008, all sensors and the communication system were renewed and a real-time monitoring system was established. In June 2010, all stations in Hagia Sophia malfunctioned as a result of lightning. They were repaired/replaced and re-installed immediately. There are occasional malfunctions taking place at different times, which are being attended soon after. In the six years since 2008, except for a few minor interruptions, the system has been working continuously and about 100 earthquakes have been recorded in Hagia Sophia.

The instrumentation in Hagia Sophia consists of nine accelerometers and four tilt-meters. Acceleration sensors have three components and currently operate at 100 Hz sampling frequency. One of the accelerometers is located at the ground level, four of them are installed at the top four main load-bearing piers and the remaining four accelerometers are located at the crowns of the four main arches, which bear the main dome. The system was operated at 200 Hz level between 16 June 2014 and 20 November 2014. However, due to software related difficulties, sampling frequency was set back to 100 Hz. Guralp CMG-

5T acceleration sensors are used at all stations. In addition to acceleration sensors, four two-component tilt-meters operating at 20 Hz are installed at stations GAL1, GAL2, GAL3 and GAL4. Tilt-meter is a measuring device that is used to monitor angular rotations of a structural element or ground. The tilt-meters were renewed on 16 November 2014 and set at 4 Hz sampling frequency. Figure 3.1 displays the location of the sensors and the station codes on a schematic representation of the structural elements of the building. Figure 3.2 shows the same information using an interior view of Hagia Sophia.

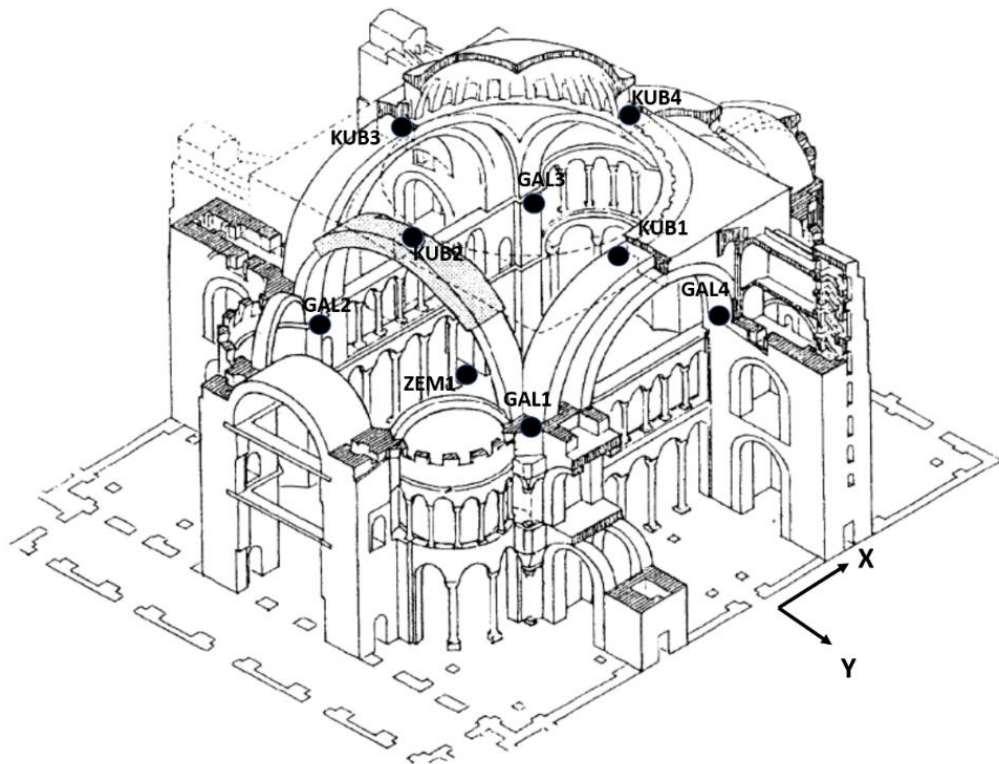


Figure 3.1. Hagia Sophia structural monitoring system; the isometric view is from Mainstone (2006).

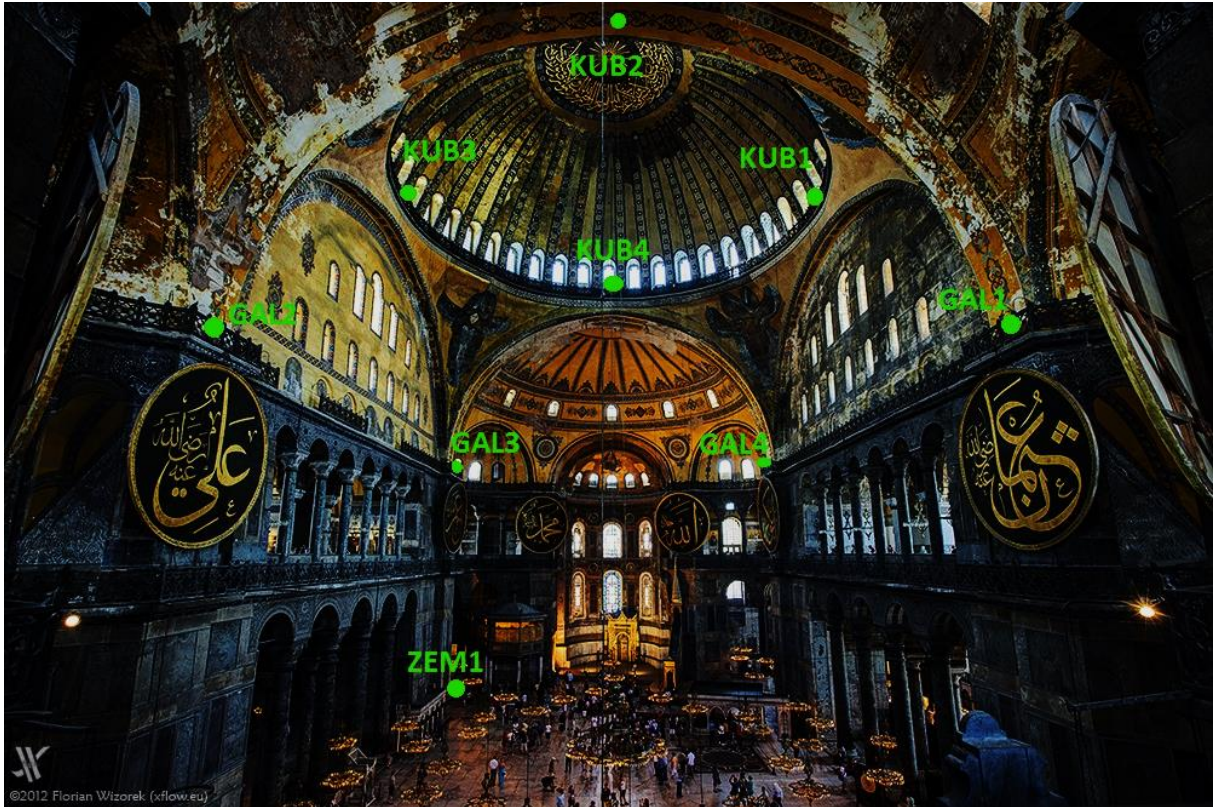


Figure 3.2. Locations of three-component accelerometric stations in Hagia Sophia. Stations GAL1, GAL2, GAL3 and GAL4 include two-way tiltmeters in addition to accelerometers.

3.2. Atmospheric Data

Structures are under continuous influence of many external factors such as ambient vibrations, earthquakes, atmospheric conditions and other human activities. One of the most important external factors is atmospheric changes. Atmospheric factors including temperature, humidity, precipitation, wind, chemicals such as chloride, salt, acid, alkali, are supposed to influence the long term performance of structures in different ways (Carden *et al.*, 2004). We use temperature, wind speed, humidity and precipitation data in this study and explore their effect on long term dynamic response of Hagia Sophia.

Atmospheric data was obtained from the General Directorate for Meteorological Affairs' (MGM) station at the Beyazıt Campus of Istanbul University, which is the nearest meteorological station to Hagia Sophia. The distance between the station and Hagia Sophia

is 1.8 km. These atmospheric data are compared with similar data obtained from Istanbul Metropolitan Municipality's Aksaray Meteorology Station, for validation. The locations of the two meteorology stations and Hagia Sophia are shown in Figure 3.3. The comparison of data obtained from two meteorology stations show that they are consistent with each other. All meteorological data are recorded as average hourly values. The time interval of the data is between 01.01.2013 and 31.12.2013.

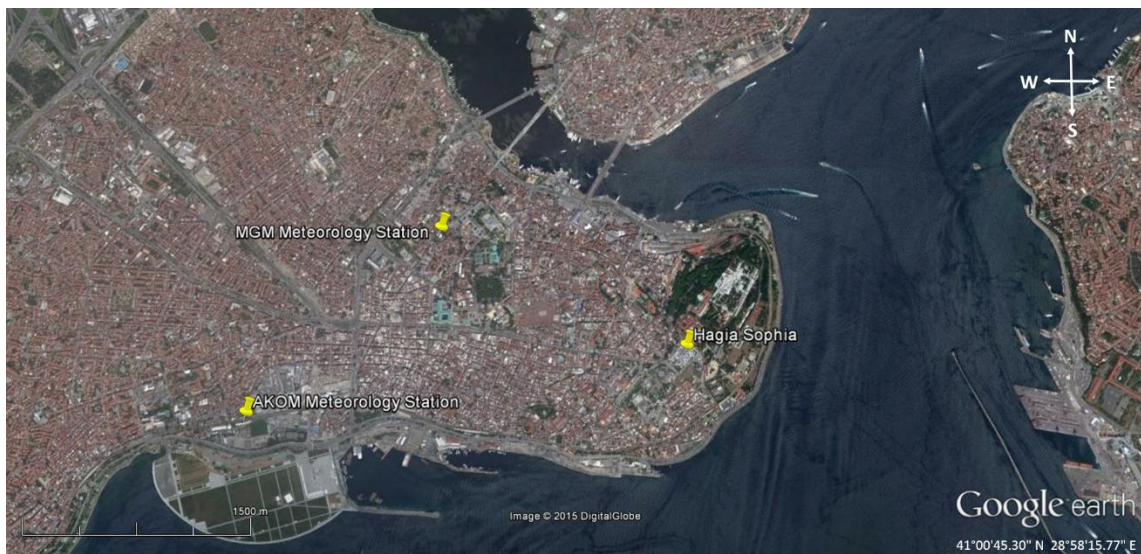


Figure 3.3. Location of Hagia Sophia in the historical peninsula of Istanbul. Also shown are the two meteorological stations the data from which are used in this study.

3.3. Earthquake Data

Hagia Sophia experienced several earthquakes with a wide range of magnitudes in the time interval between 2008 and 2015. In this time period, more than a hundred earthquakes were recorded by Hagia Sophia vibration monitoring system. Sixty three of these earthquakes, with the majority of them occurring between 2012 and 2014 are considered in this study.

In the database, there are gaps in some of the recorded earthquakes. During thirteen earthquakes, one or two stations did not record the earthquake due to technical problems. In addition, the sensor at station KUB3 had a problem in Y direction except in one earthquake. All these problems are fixed and all recordings are evaluated according to their particular circumstances.

There are four earthquakes in the database having magnitudes larger than six. Two of them are associated with the largest accelerations recorded in Hagia Sophia. Both of them took place at more than 300 km epicentral distance. The largest ground motion recorded at Hagia Sophia is due to the Aegean Sea Earthquake on 24 May 2014 with 6.5 M_L and 305 km epicentral distance. The second largest earthquake was again at Aegean Sea that occurred on 8 January 2013 with 6.2 M_L and 332 km away. The farthest recorded event was the 23 November 2011 Van Earthquake with 6.6 M_L at an epicentral distance of 1257 km to Hagia Sophia. The sampling rates of earthquakes are not identical. Thirteen of the earthquakes were recorded with 200 Hz while fifty of them were recorded at 100 Hz. Earthquakes in the database are shown on the map in Figure 3.4 and Figure 3.5 Their epicentral properties and peak accelerations at ground level are shown in Tables 3.1, 3.2, 3.3 and 3.4. The epicentral information is from <http://udim.koeri.boun.edu.tr/indexeng.htm>.



Figure 3.4. Epicenters of earthquakes recorded in Hagia Sophia. Yellow flag indicates the location of Hagia Sophia.

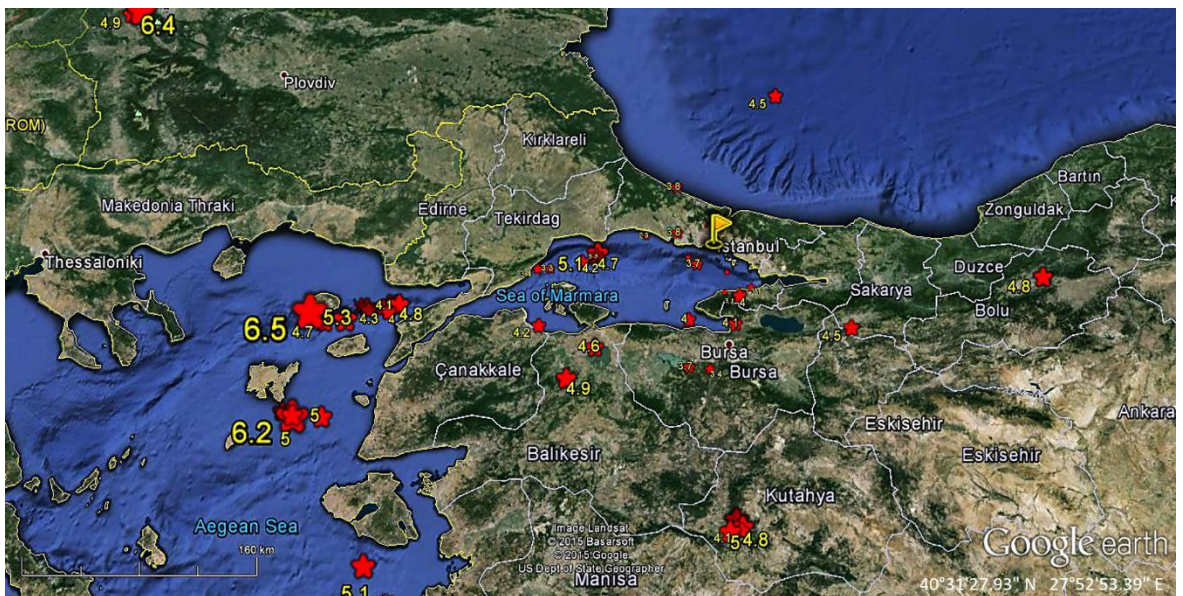


Figure 3.5. Epicenters of earthquakes in the Marmara region recorded in Hagia Sophia (essentially a close-up of Figure 3.3). Yellow flag indicates the location of Hagia Sophia.

Table 3.1. Earthquakes recorded in the time interval between 2008 and 2012 in Hagia Sophia.

Event Date (dd.mm.yy)	Time (Local)	Event Coordinates		Depth (km)	Event Location	Magnitude (M_L)	Distance (km)	Acceleration (cm/sn^2)		
		Longitude	Latitude					Zeml X	Zeml Y	Zeml Z
10.07.2008	10:49:53	39.995	27.7037	13.2	Balikesir	4.9	156	0.45	0.86	0.24
24.01.2009	17:58:38	40.798	27.785	11.2	Marmara Sea	4.2	103	0.21	0.24	0.11
17.02.2009	07:28:19	39.1067	29.0392	7.3	Simav (Kütahya)	5	211	0.29	0.22	0.16
21.10.2011	08:12:27	40.8405	27.901	13.2	Marmara Sea	3.2	92	0.04	0.05	0.03
23.10.2011	13:41:20	38.726	43.427	5	Tabanlı (Van)	6.6	1257	0.01	0.00	0.00
05.12.2011	10:17:26	38.8097	26.2345	6	Aegean Sea	5.1	338	0.07	0.07	0.04
14.03.2012	11:24:54	40.8158	28.7973	7.7	Marmara Sea	3.7	26	0.47	0.34	0.21
16.04.2012	13:10:46	39.1365	29.1387	5	Simav (Kütahya)	4.8	208	0.07	0.08	0.03
03.05.2012	18:20:25	39.1747	29.0918	3.1	Hisarcık (Kütahya)	5.1	204	0.19	0.15	0.11
22.05.2012	03:00:33	42.606	23.0912	28.1	Bulgaria	6.4	519	0.11	0.17	0.09
22.05.2012	04:30:49	42.5943	22.9903	3.5	Bulgaria	4.9	526	0.00	0.01	0.00
07.06.2012	23:54:25	40.8483	27.921	14.9	Marmara Sea	5.1	90	0.45	0.51	0.24
10.06.2012	15:44:16	36.4542	28.9047	19.4	Mediterranean Sea	6	506	0.07	0.06	0.03
26.07.2012	00:28:28	40.4317	26.1942	14.5	Saros Gulf	4.6	243	0.07	0.08	0.05
19.10.2012	11:17:24	41.0347	28.6255	13.2	Büyükçekmece (İstanbul)	3.8	29	0.37	0.41	0.30

Table 3.2. Earthquakes recorded in 2013 in Hagia Sophia.

<i>Event Date (dd.mm.yy)</i>	<i>Time (Local)</i>	<i>Event Coordinates</i>		<i>Depth (km)</i>	<i>Event Location</i>	<i>Magnitude (M_L)</i>	<i>Distance (km)</i>	<i>Acceleration (cm/sn²)</i>		
		<i>Longitude</i>	<i>Latitude</i>					<i>Zem1 X</i>	<i>Zem1 Y</i>	<i>Zem1 Z</i>
08.01.2013	16:16:06	39.6462	25.4833	8.4	Aegean Sea	6.2	332	0.92	1.20	0.63
09.01.2013	17:41:33	39.6713	25.7202	6.4	Aegean Sea	5.0	313	0.08	0.11	0.05
11.01.2013	02:30:18	39.6935	25.3855	9	Aegean Sea	4.6	337	0.02	0.03	0.01
11.01.2013	23:56:15	40.4202	25.898	14.6	Saros Gulf	4.2	267	0.02	0.02	0.02
13.01.2013	10:55:13	39.6705	25.4747	9.5	Aegean Sea	5.0	332	0.03	0.03	0.02
19.03.2013	14:44:30	42.129	29.5792	10.7	Black Sea	4.5	134			
12.07.2013	03:36:57	40.3837	25.965	13.2	Saros Gulf	4.3	263			
30.07.2013	08:33:08	40.3037	25.7803	9.8	Gökçeada (Çanakkale)	5.3	281	0.22	0.27	0.17
17.08.2013	21:16:31	40.4095	29.1213	5.7	Gemlik (Bursa)	4.1	67	0.09	0.08	0.05
29.08.2013	09:20:34	40.3423	27.4427	14.1	Biga (Çanakkale)	4.2	149	0.07	0.10	0.06
03.10.2013	13:26:07	40.113	28.7238	2.3	Nilufer (Bursa)	3.7	102	0.03	0.03	0.02
24.11.2013	22:49:37	40.7843	31.876	8	Ulumescit (Bolu)	4.8	244	0.08	0.07	0.07
27.11.2013	06:13:37	40.851	27.9198	9.6	Marmara Sea	4.7	90	0.26	0.29	0.15
27.11.2013	06:21:35	40.847	27.912	7.4	Marmara Sea	4.0	91	0.10	0.14	0.06

Table 3.3. Earthquakes recorded in first six months of 2014 in Hagia Sophia.

<i>Event Date (dd.mm.yy)</i>	<i>Time (Local)</i>	<i>Event Coordinates</i>		<i>Depth (km)</i>	<i>Event Location</i>	<i>Magnitude (M_L)</i>	<i>Distance (km)</i>	<i>Acceleration (cm/sn²)</i>		
		<i>Longitude</i>	<i>Latitude</i>					<i>Zem1 X</i>	<i>Zem1 Y</i>	<i>Zem1 Z</i>
30.01.2014	04:54:33	40.6733	29.2688	8.5	Yalova	3.1	44	0.06	0.11	0.07
05.02.2014	03:56:43	41.3768	28.622	16	Arnavutköy (Istanbul)	3.8	50	0.63	0.38	0.23
27.03.2014	20:20:08	41.0095	28.3462	8.4	Marmara Sea	2.9	53	0.06	0.04	0.02
04.04.2014	05:52:05	40.6348	29.0363	7.4	Çınarcık (Yalova)	2.5	41	0.01	0.01	0.00
07.04.2014	12:51:02	41.1043	28.8817	5.2	Sultangazı (Istanbul)	2.1	15	0.01	0.02	0.02
07.04.2014	04:25:45	40.8727	28.7187	20.7	Avcılar (Istanbul)	2.5	26	0.01	0.02	0.04
24.05.2014	12:25:01	40.3242	25.4687	23.3	Aegean Sea	6.5	305	3.11	2.69	1.96
24.05.2014	14:33:07	40.284	25.6083	4.9	Aegean Sea	4.7	295	0.04	0.04	0.02
24.05.2014	12:31:18	40.4305	26.2267	7.8	Saros Gulf	4.8	241	0.04	0.04	0.03
24.05.2014	13:11:40	40.3892	26.1418	9	Saros Gulf	4.3	249	0.03	0.04	0.02
24.05.2014	13:35:00	40.4247	26.1357	1.3	Saros Gulf	4.1	248	0.02	0.02	0.01
24.05.2014	18:01:32	40.3795	26.1425	9.2	Saros Gulf	4.0	249	0.01	0.02	0.01
24.05.2014	17:49:14	40.4013	25.9517	2.1	Saros Gulf	4.6	264	0.00	0.00	0.01
25.05.2014	14:38:38	40.4235	26.1442	13.1	Saros Gulf	4.8	247	0.27	0.27	0.23
25.05.2014	14:47:55	40.4103	26.0895	6.8	Saros Gulf	4.5	252	0.04	0.04	0.03
25.05.2014	02:00:35	40.4048	25.9343	10.2	Saros Gulf	4.2	265	0.02	0.03	0.02
25.05.2014	08:44:22	40.4165	26.0518	13.5	Saros Gulf	3.9	255	0.01	0.01	0.00
28.05.2014	06:59:51	40.422	26.14	13.3	Saros Gulf	4.5	248	0.04	0.04	0.03
30.06.2014	21:32:23	40.1073	28.8985	6.6	Nilufer (Bursa)	3.4	100	0.02	0.03	0.01

Table 3.4. Earthquakes recorded in last six months of 2014 in Hagia Sophia.

<i>Event Date (dd.mm.yy)</i>	<i>Time (Local)</i>	<i>Event Coordinates</i>		<i>Depth (km)</i>	<i>Event Location</i>	<i>Magnitude (ML)</i>	<i>Distance (km)</i>	<i>Acceleration (cm/sn²)</i>		
		<i>Longitude</i>	<i>Latitude</i>					<i>Zeml X</i>	<i>Zeml Y</i>	<i>Zeml Z</i>
03.07.2014	08:04:46	40.2083	27.9282	12.1	Manyas (Balıkesir)	4.6	125	0.23	0.34	0.21
03.08.2014	13:42:44	40.6045	29.157	6	Termal (Yalova)	3.6	47	0.05	0.04	0.03
03.08.2014	16:20:22	40.6085	29.1752	5.3	Termal (Yalova)	3.1	47	0.02	0.03	0.01
03.08.2014	10:48:39	40.6027	29.1642	4.9	Termal (Yalova)	3.1	47	0.02	0.02	0.01
03.08.2014	16:37:48	40.6055	29.1778	5.1	Termal (Yalova)	3.0	47	0.01	0.02	0.01
04.08.2014	01:22:44	40.6025	29.1655	10.7	Termal (Yalova)	4	47	0.15	0.18	0.10
16.09.2014	10:19:48	40.7768	29.0608	6.5	Marmara Sea	2.8	26	0.05	0.07	0.02
24.09.2014	07:44:27	40.8327	28.7603	1.9	Marmara Sea	2.6	27	0.04	0.04	0.02
08.10.2014	06:08:49	40.7437	27.5082	13.1	Marmara Sea	3.3	127	0.02	0.03	0.01
22.10.2014	20:11:05	40.4047	30.1188	7.6	Geyve (Sakarya)	4.5	117	0.37	0.22	0.20
23.10.2014	17:53:50	40.7373	27.398	8.5	Marmara Sea	3.4	136	0.01	0.01	0.01
12.11.2014	21:14:15	45.742	27.2147	27.9	Romania	5.6	445	0.46	0.28	0.10
28.11.2014	04:30:06	39.3512	29.018	5.3	Sınav (Kütahya)	4.5	184	0.09	0.06	0.03

3.4. Data Processing

Recorded data do not represent the actual response of structures in most cases. This raw data need to be processed in order to achieve a reliable extraction of structure-related information.

Data were prepared and processed differently for the investigation of atmospheric effects and for the analysis of earthquake recordings. For the investigation of correlation between modal parameters and atmospheric conditions, we needed to look at one-year long data from 24 channels (8 stations at the upper levels in Hagia Sophia with sensors in three components) to be able to deduce daily, monthly and seasonal changes. For the analysis of earthquake specific data, typical recording lengths were in the order of tens of seconds.

For the analysis associated with atmospheric effects, first and second modal frequencies of vibration and corresponding damping values need to be identified. For earthquake specific analysis, in addition to first and second modal frequencies of vibration, modal shapes associated with them; peak accelerations, velocities and displacements during each earthquake throughout the structure are also determined.

To prepare the data for the assessment of long-term frequency variation of Hagia Sophia over one year period following steps are taken. The continuous data from the 27 channels of acceleration sensors are stored on a daily basis. The sampling rate of these data is 100 Hz. First daily data are combined and turned into weekly data. As the data size becomes very large during this process and slows down any processing and analysis considerably, the data are decimated by 5, decreasing the sampling frequency from 100 Hz to 20 Hz. Reduction of the sampling rate decreases the processing time and does not change the results as well, since the modal frequencies of interest lie in the frequency range between 1.5 and 2.5 Hz. In addition, there is no need for additional filtering to eliminate the noise at high frequencies occurring typically at frequencies larger than 15 to 20 Hz, as the Nyquist frequency becomes 10 Hz.

After the data are prepared, in the third phase, base line correction is applied by removing the mean value or linear trend from the data. The mean of acceleration and velocity data is expected to be zero. In case, these values are not equal to zero, displacement values can be completely unrealistic. It means that the base line of recorded data is not at zero level. To overcome this problem, the mean or linear trend is subtracted from data.

In the next phase, Short Time Fourier Transform (STFT) analysis is applied. STFT divides signal into windows with overlaps and estimates Fast Fourier amplitude for each window that moves with time. By means of this process, changes in the predominant frequency of a structure can be tracked. At this stage, identification of window length and overlapping length are essential. In this study, window length and overlapping length are selected as 60 minutes and 30 minutes respectively.

In the next stage, the variation of predominant frequency in time domain (week long data in this case) is smoothed to eliminate unrealistic peaks. Next is smoothing of the Fourier amplitude spectrum for a better and easier identification of the predominant frequency. In some cases, unrealistic peaks can be seen in Fourier amplitude spectrum due to environmental conditions and mechanical imperfections in the instruments. In addition to unrealistic peaks, the jags on Fourier amplitude spectrum can lead to miscalculation of the predominant frequency. Smoothing the Fourier amplitude spectrum is a good solution to obtain most accurate frequency values. However, extreme smoothing can flatten out all peaks. Therefore, smoothing should be done very carefully to obtain accurate frequency values.

As the final step, identified frequencies in weekly periods (52 of them) are combined to yield yearly data. The phases of processing of this year-long data are presented as a diagram in Figure 3.6.

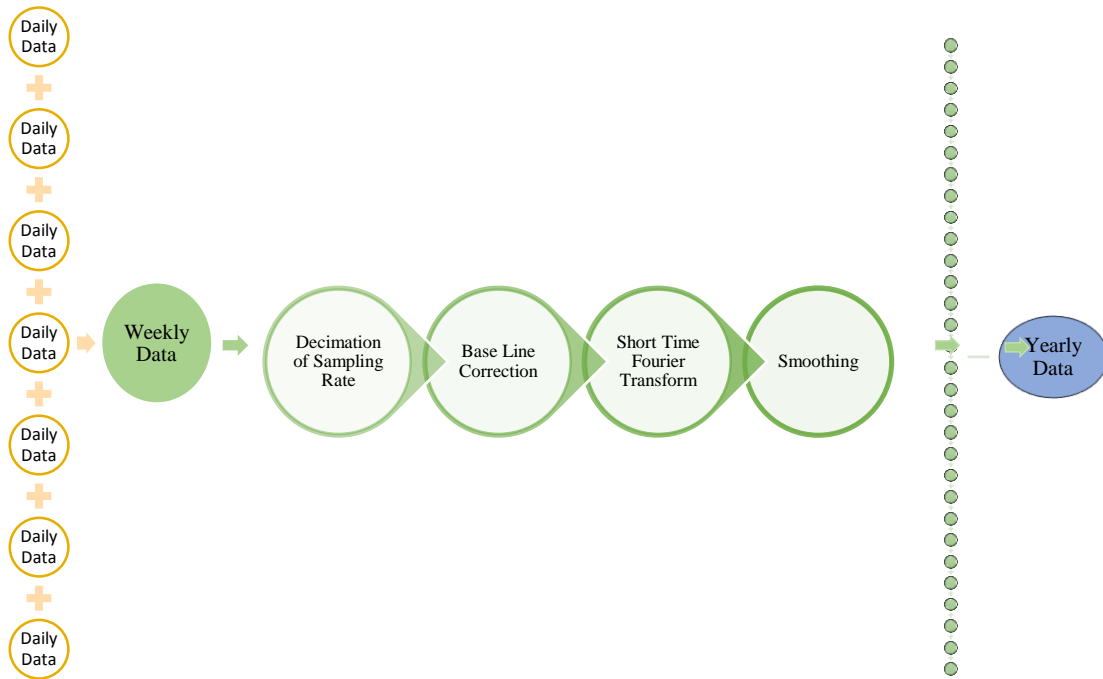


Figure 3.6. Steps for preparation and analysis of data for long term analysis.

Processing of recordings of single earthquakes involved baseline correction, band pass filtering, estimation of Fourier amplitude spectrum, its smoothing for the identification of predominant frequencies, estimation of corrected velocities and displacements, estimation of peak accelerations, velocities and displacements, and estimation of particle motions narrow-band filtered for predominant frequencies. The sampling rate is 100 Hz.

4. EFFECT OF ATMOSPHERIC CONDITIONS ON MODAL FREQUENCY AND MODAL DAMPING

4.1. Temperature

Research shows that among all atmospheric conditions, temperature has the largest influence on the dynamic behavior of structures (Gueguen *et al.*, 2014; Alampalli, 1998; Ramos *et al.*, 2010; Martins *et al.*, 2014; Chang *et al.*, 2003). In this section, we explore whether there is any correlation between the temperature and the modal frequencies of Hagia Sophia using data from year 2013.

Two gallery level stations, GAL1 and GAL2, and two dome level stations, KUB1 and KUB2 are selected. It is anticipated that stations GAL3, GAL4, KUB3 and KUB4 will yield results similar to the selected ones. Figures 4.1, 4.2, 4.3 and 4.4 show temperature and first modal frequency as a function of time at stations GAL1, GAL2, KUB1 and KUB2 respectively. In Figure 4.5 through Figure 4.8, the temperature and second modal frequency are co-plotted as a function of time at the same stations. From these figures, it can be clearly seen that temperature has a great influence on the modal frequencies of Hagia Sophia. Both frequencies increase with the rise of temperature in the transition from winter to summer and decrease with the temperature drop towards winter months. In December, January and February they remain more or less constant (1.73 Hz as the first modal frequency and 2.02 Hz as the second modal frequency). From March, they steadily increase to 1.9 Hz and 2.17 Hz respectively in mid-August, followed by a steady decrease. The change in frequency is 9.8% for the first mode and 7.4% for the second mode.

The figures show that frequency is not only sensitive to long-term temperature variations across the seasons, but also to temperature changes within a month and even within one day. The dependence of modal frequencies to temperature changes within a month can already be observed in Figure 4.1 through Figure 4.8 and exists in all months of 2013. In order to observe daily frequency variation with temperature, it is better to choose a period

of time where other environmental effects can be neglected. For this purpose, we have selected the period between 14 -26 June 2013, since other atmospheric factors such as wind and rain was not observed in these days. Figure 4.9 and Figure 4.10 show temperature and modal frequencies in this time interval at station KUB1 in two orthogonal directions, indicating the clear dependence between the two parameters. However there are periods of time where this dependence is not that obvious as shown in Figure 4.11 and Figure 4.12, where the two parameters are shown in the first half of February 2013.

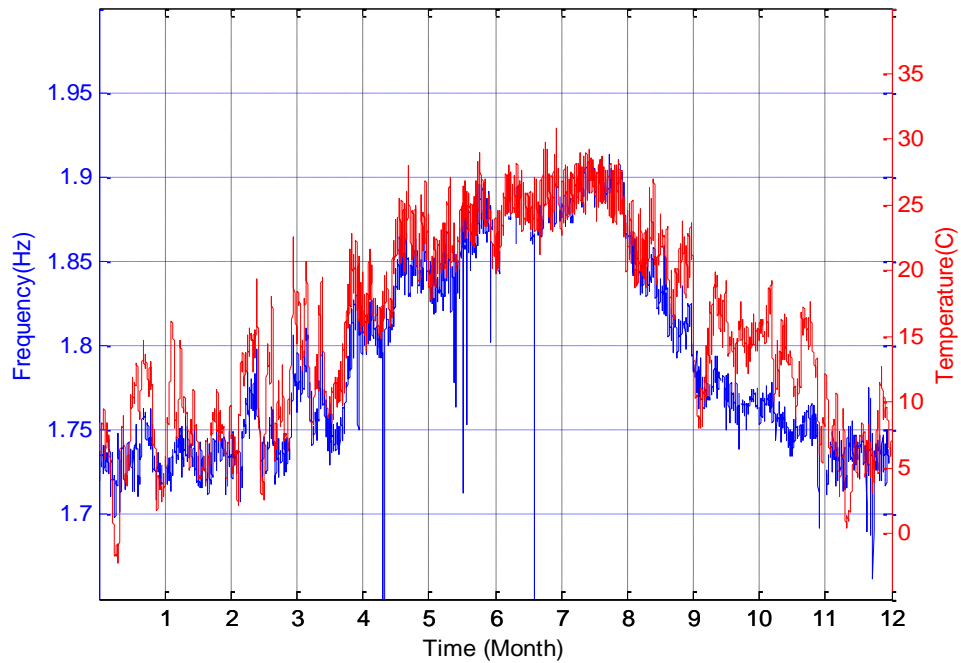


Figure 4.1. Variation of first modal frequency at station GAL1 and temperature in year 2013 (X direction).

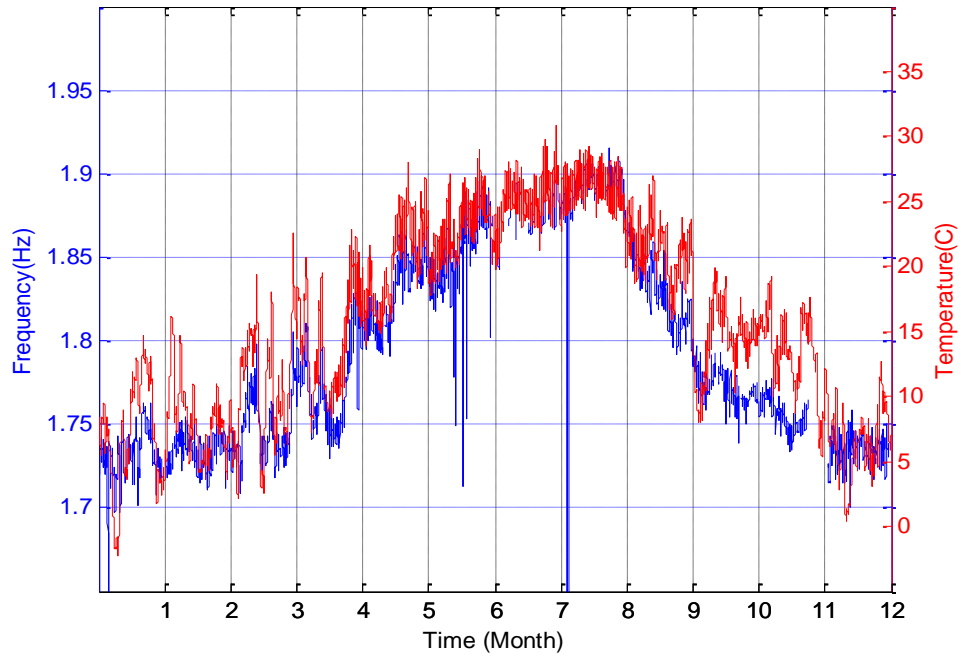


Figure 4.2. Variation of first modal frequency at station GAL2 and temperature in year 2013 (X direction).

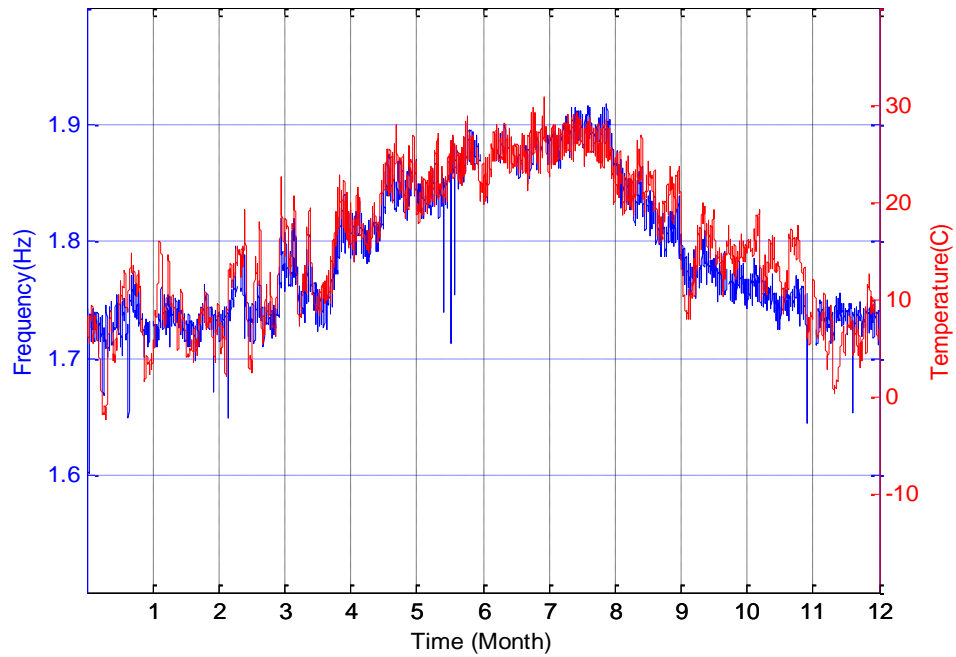


Figure 4.3. Variation of first modal frequency at station KUB1 and temperature in year 2013 (X direction).

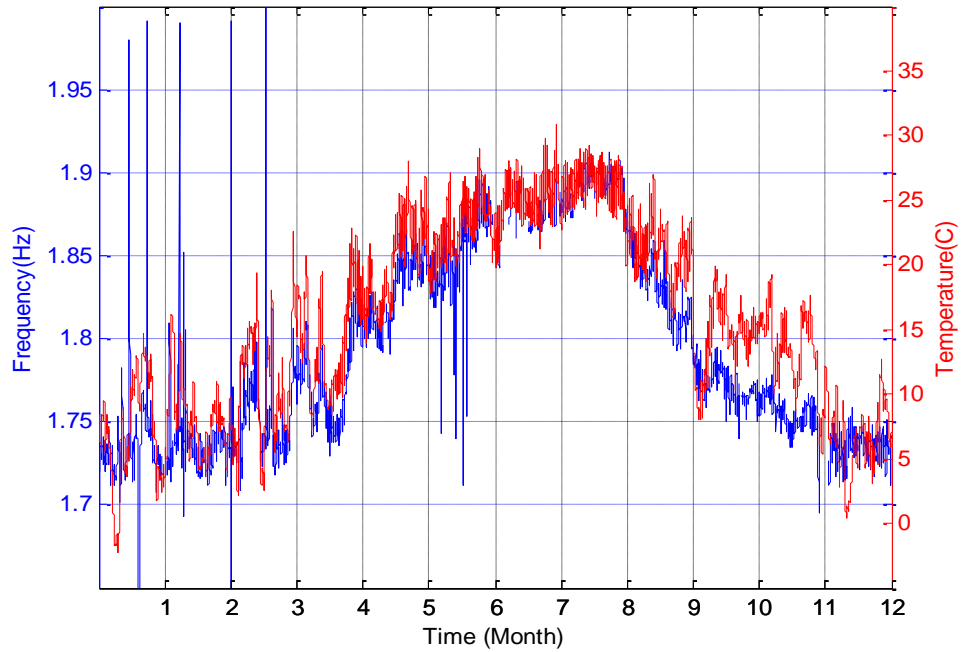


Figure 4.4. Variation of first modal frequency at station KUB2 and temperature in year 2013 (X direction).

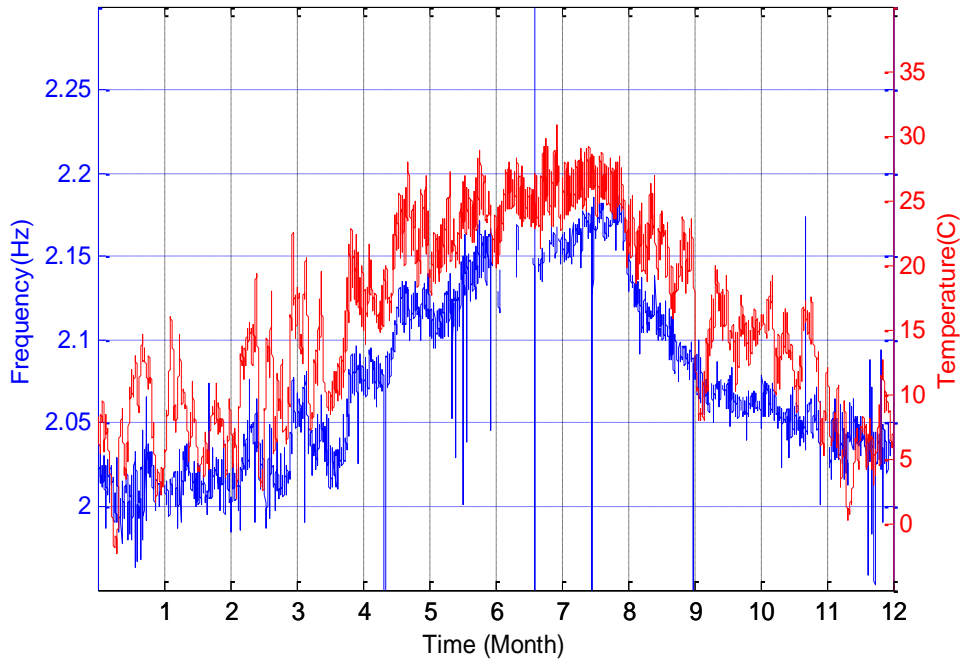


Figure 4.5. Variation of second modal frequency at station GAL1 and temperature in year 2013 (Y direction).

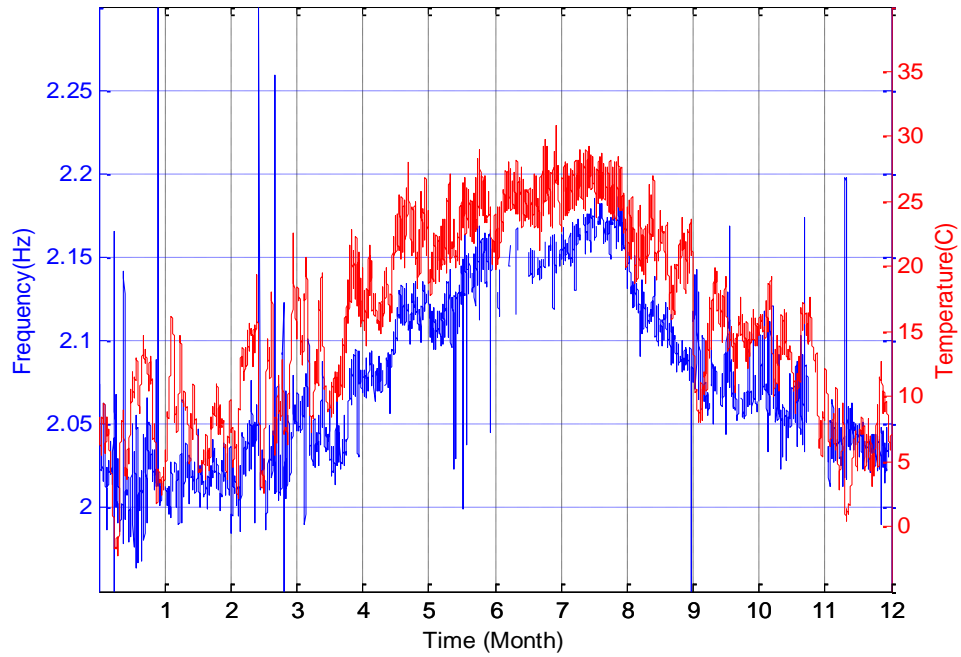


Figure 4.6. Variation of second modal frequency at station GAL2 and temperature in year 2013 (Y direction).

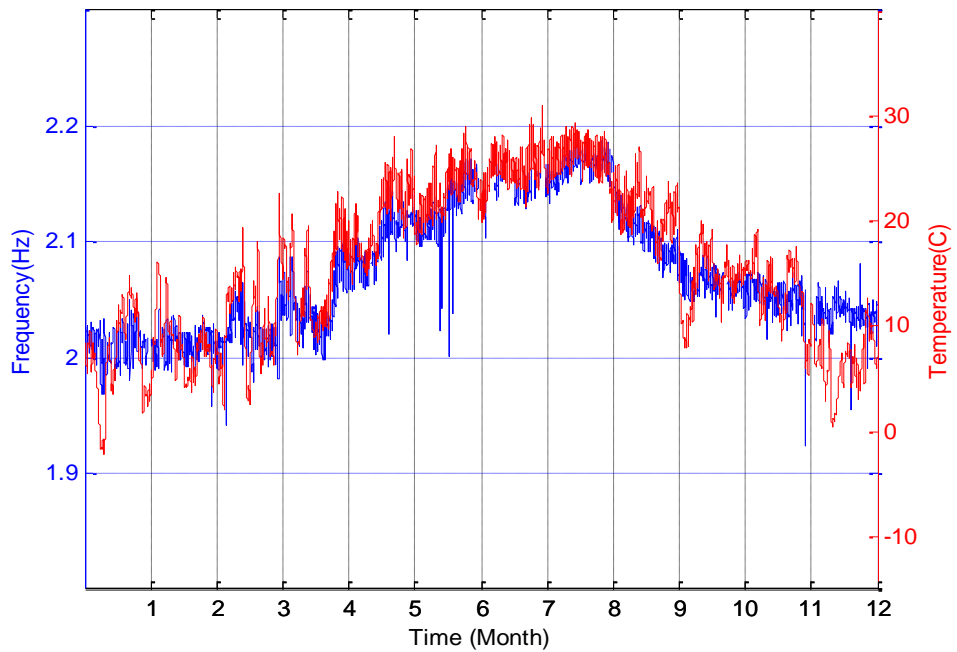


Figure 4.7. Variation of second modal frequency at station KUB1 and temperature in year 2013 (Y direction).

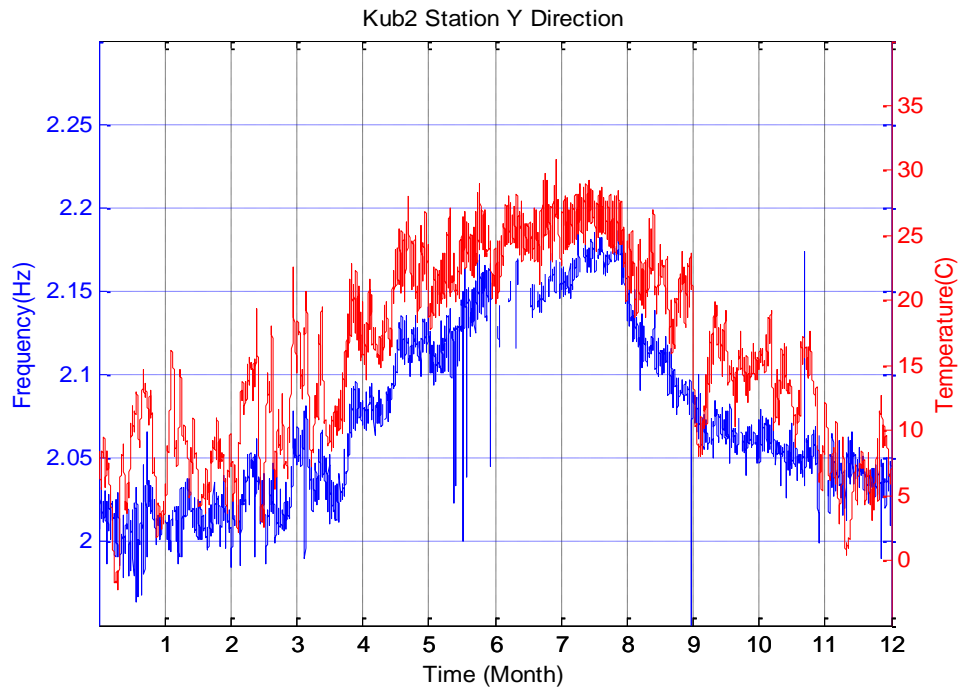


Figure 4.8. Variation of second modal frequency at station KUB2 and temperature in year 2013 (Y direction).

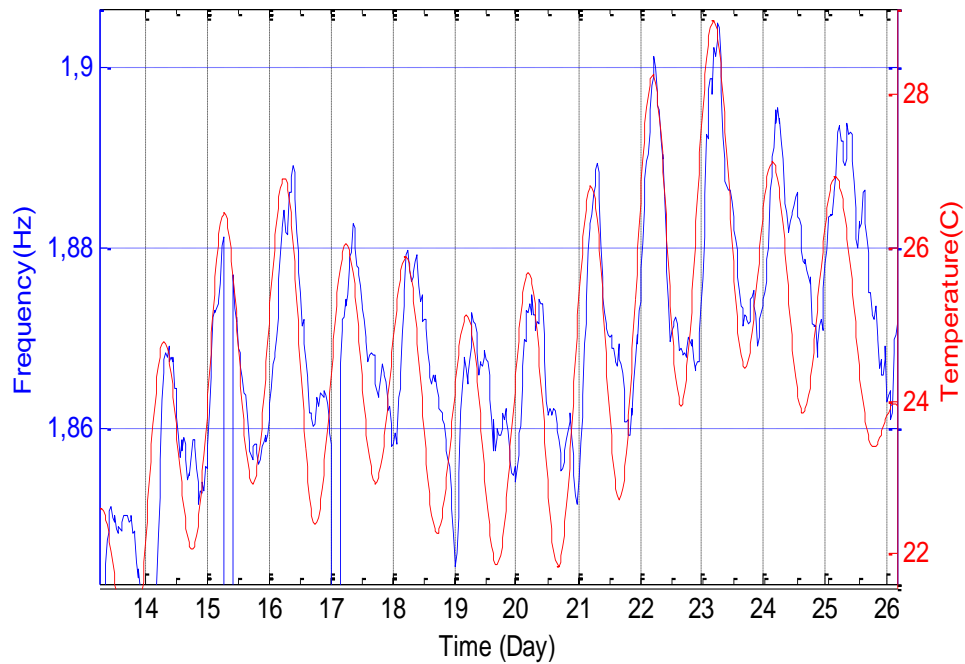


Figure 4.9. Variation of first modal frequency at station KUB1 and temperature between 13.06.2013 and 26.06.2013 (X direction).

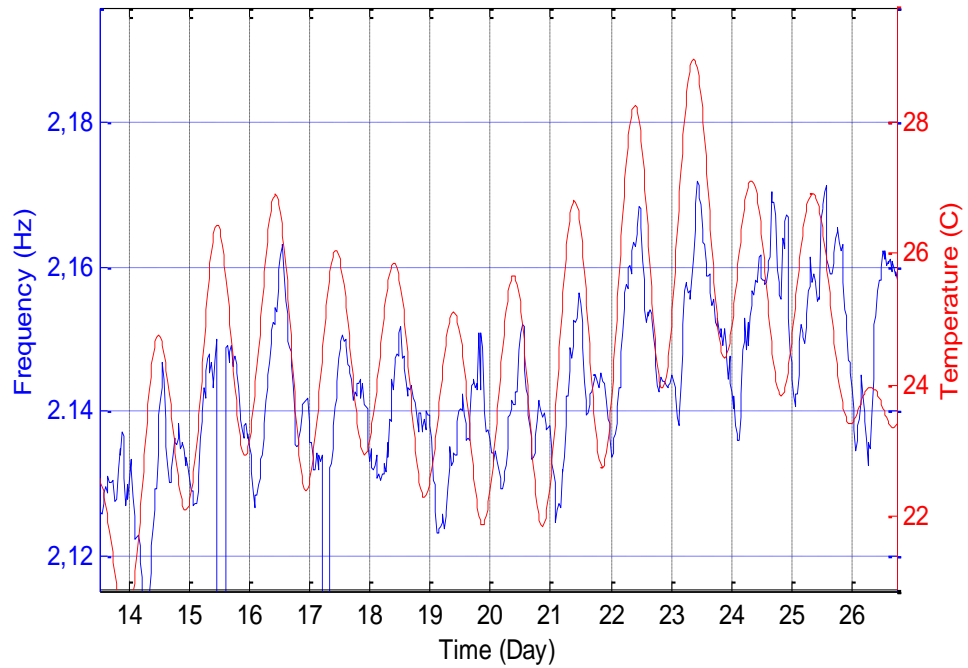


Figure 4.10. Variation of second modal frequency at station KUB1 and temperature between 13.06.2013 and 26.06.2013 (Y direction).

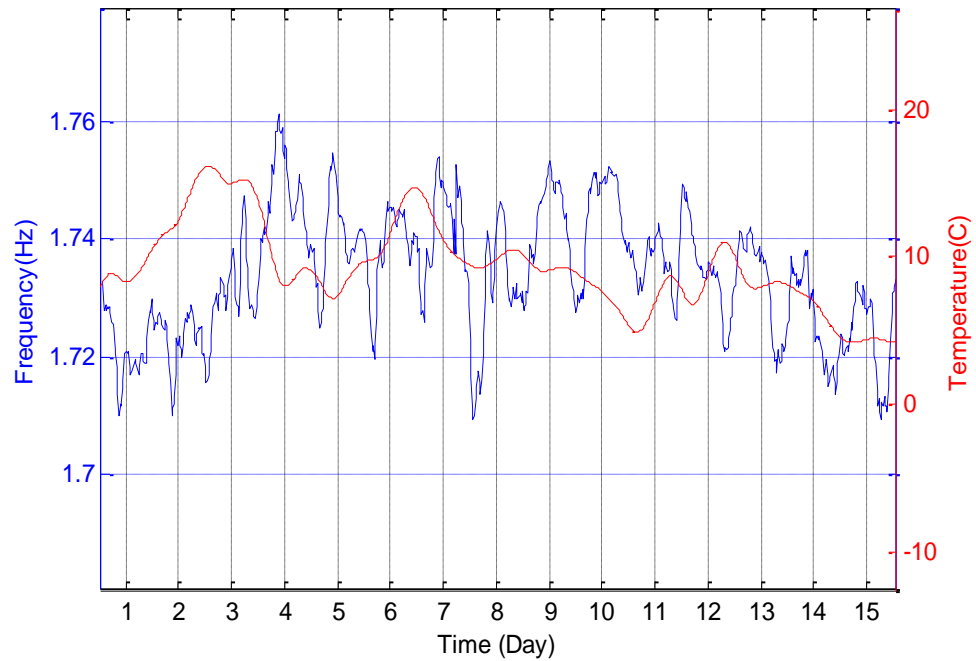


Figure 4.11. Variation of second modal frequency at station KUB1 and temperature during the first 15 days of February 2013 (X direction).

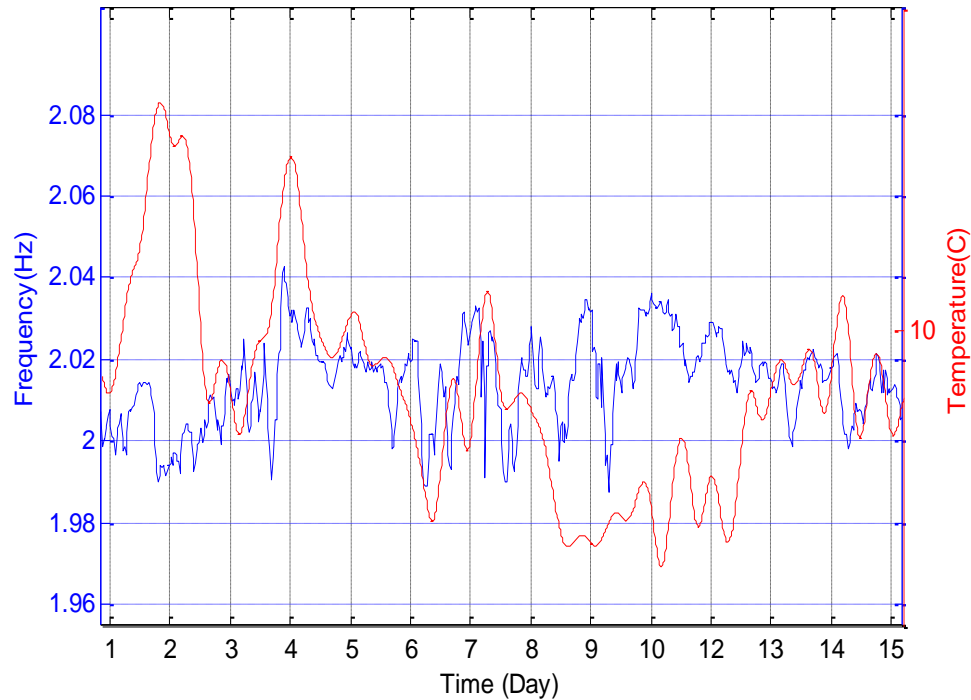


Figure 4.12. Variation of second modal frequency at station KUB1 and temperature during the first 15 days of February 2013 (Y direction).

It appears that also damping is correlated with temperature. Variation in damping is compared with temperature over one year period. Damping values are taken from KOERI-MIDS coded for Hagia Sophia for the analysis of continuous vibration data (Kaya and Safak, 2009). The software estimates damping ratio as a mean of all channels. Estimates of damping in 2013 were not uninterrupted. Yet they were good enough to observe their trend. Similar to modal frequencies, damping ratio is also directly related to temperature. The increase in temperature decreases the modal damping ratio of the structure. Figure 4.13 and Figure 4.14 show the relationship between modal damping ratio of the structure and temperature associated with first and second modal shapes respectively. The damping drops from about 2.95% in winter, to about 2.65% in summer in the first mode. In the second mode the drop is from about 3.5% to 3.15%. This means a difference of about 10% for the two modes.

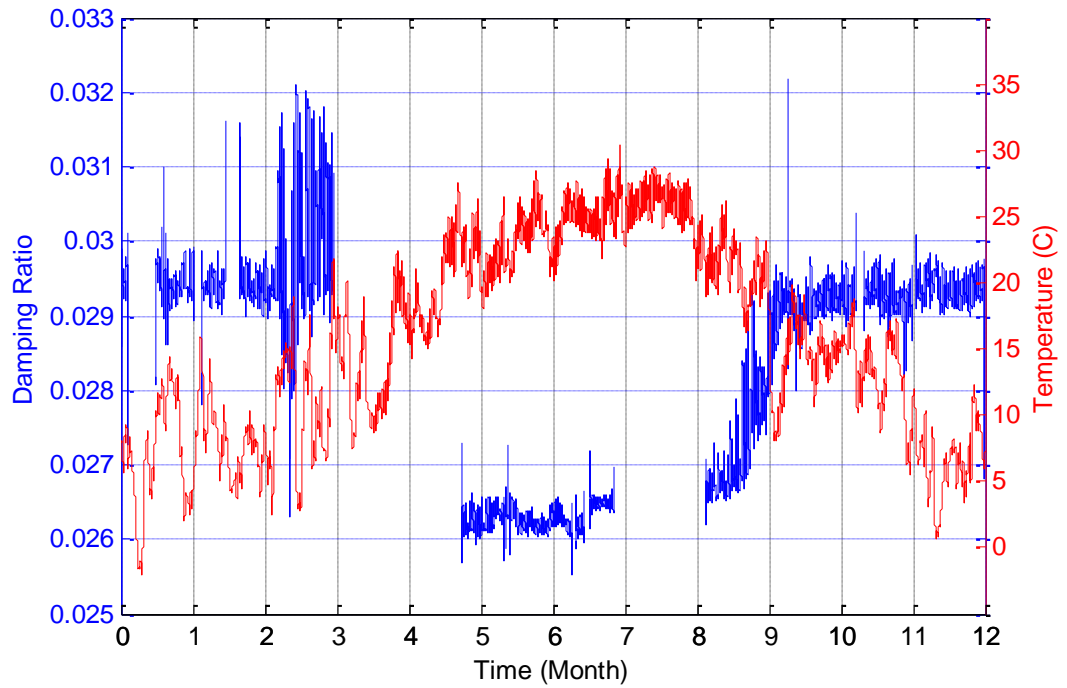


Figure 4.13. Variation of mean damping ratio and temperature in year 2013 (X direction).

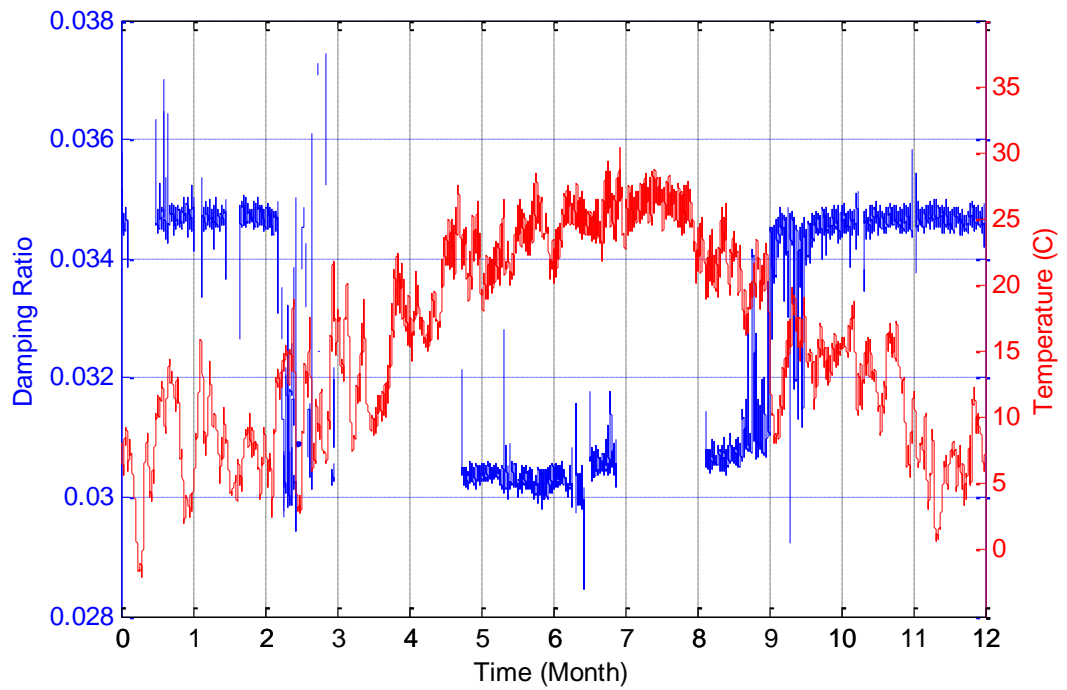


Figure 4.14. Variation of mean damping ratio and temperature in year 2013 (Y direction).

4.2. Wind

In the last 50 years, many developments took place in wind engineering in order to characterize the effect of wind on structures. Recent studies show that wind and earthquake have similar impact on dynamic behavior of structures (Martins *et al.*, 2014; Ou and Li, 2010; Davenport, 1961; Holmes, 2001). Both of these natural phenomena impose dominant loads on the structure and may lead to severe damages. It is known that tall buildings and bridges are more vulnerable to wind compared to other types of structures.

In this section, influence of wind speed on modal parameters is described by the examination of relationship between average hourly wind speed and ambient vibration characteristics of the structure. The direction of wind is not taken into consideration due to the fact that wind direction changes momentarily and it is too difficult to evaluate wind direction in one-year time interval. Therefore, we observe only the effect of wind speed on Hagia Sophia.

Wind applies mostly lateral loads to structures similar to earthquake excitation. It has been shown that even during small amplitude ground accelerations the modal frequencies of Hagia Sophia tend to drop (Durukal *et al.*, 2003), probably true for other historical masonry structures as well. The fact that lateral loads increase the period of masonry structures and decrease the frequency, was attributed to the widespread existence of micro-cracking in masonry. Therefore it is reasonable to expect that in contrast to temperature, wind may cause a decrease in natural vibration frequency of masonry structures. However wind is an instantaneously altering effect unlike temperature. Hence, it is too difficult to observe a relationship between wind and frequency in annual time interval. Figure 4.15 and Figure 4.16 show the annual variation of frequency and wind speed in X and Y directions respectively.

Considering a daily time interval in a period of the year where the influence of temperature on frequency is not as pronounced and the wind speeds are relatively high, a remarkable detail stands out; there is a prevailing game between wind and temperature. Two

opposite effects try to be superior to each other. While the increase in temperature causes the modal frequency of the structure to rise, strong winds drop it rapidly. When the wind is strong, it breaks the domination of temperature control on frequency and results in its instantaneous decrease. This phenomenon is shown in Figure 4.17 and Figure 4.18 for a time period in January 2013.

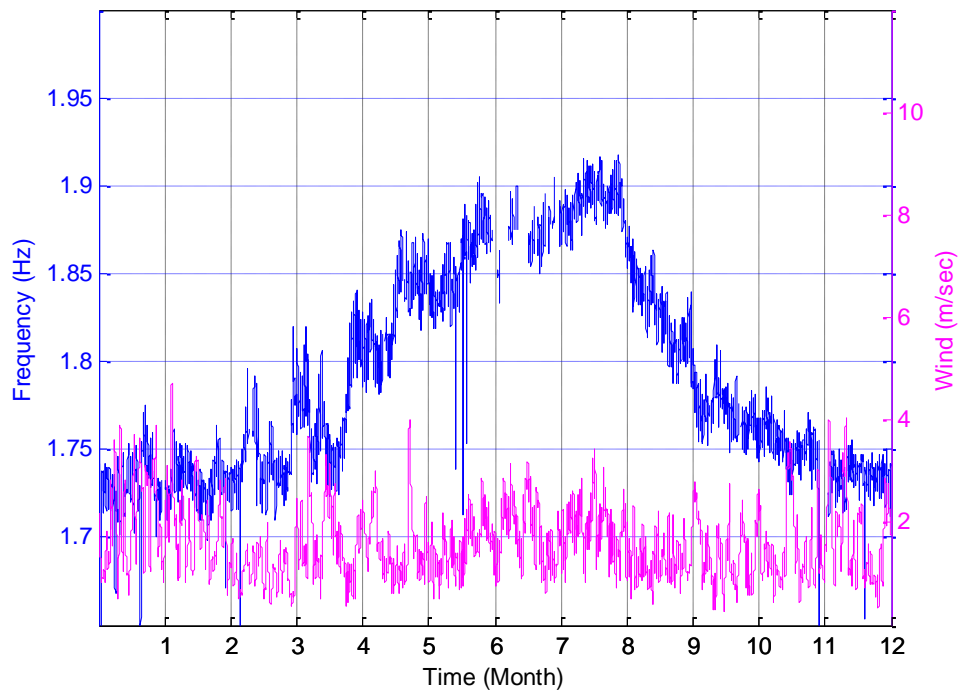


Figure 4.15. Variation of first modal frequency at station KUB1 and wind speed in year 2013 (in X direction).

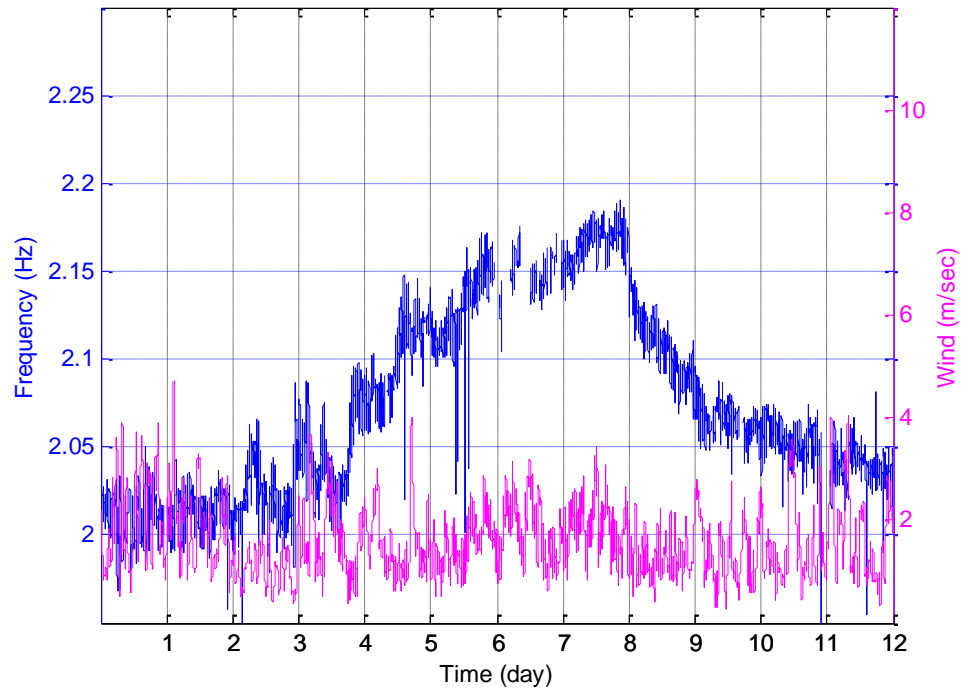


Figure 4.16. Variation of second modal frequency at station KUB1 and wind speed in year 2013 (in Y direction).

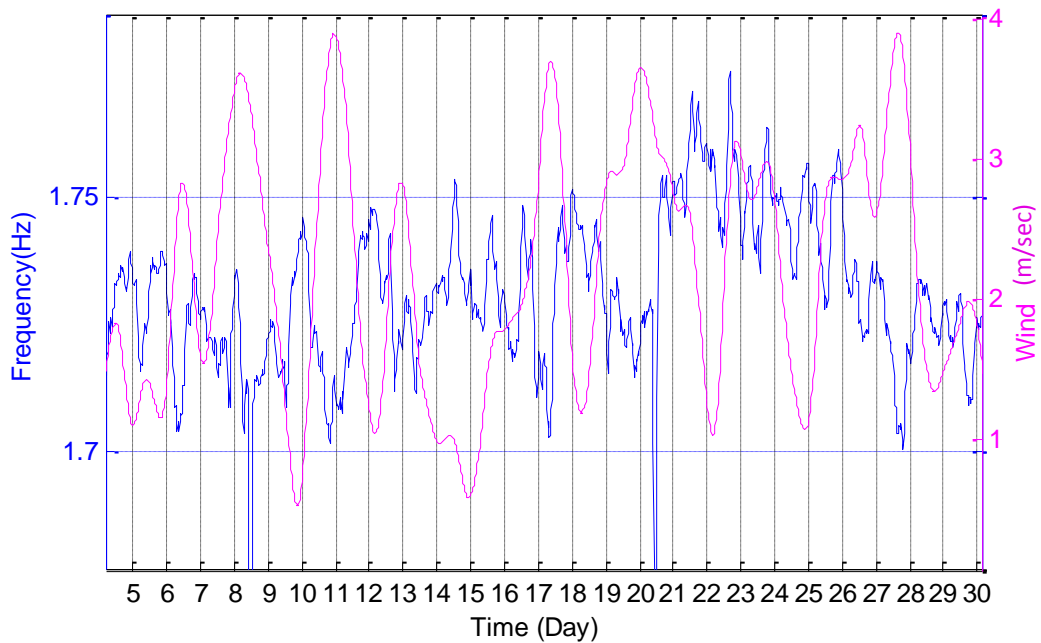


Figure 4.17. Variation of first modal frequency at station KUB1 and wind speed between 04.01.2013 and 30.01.2013 (in X direction).

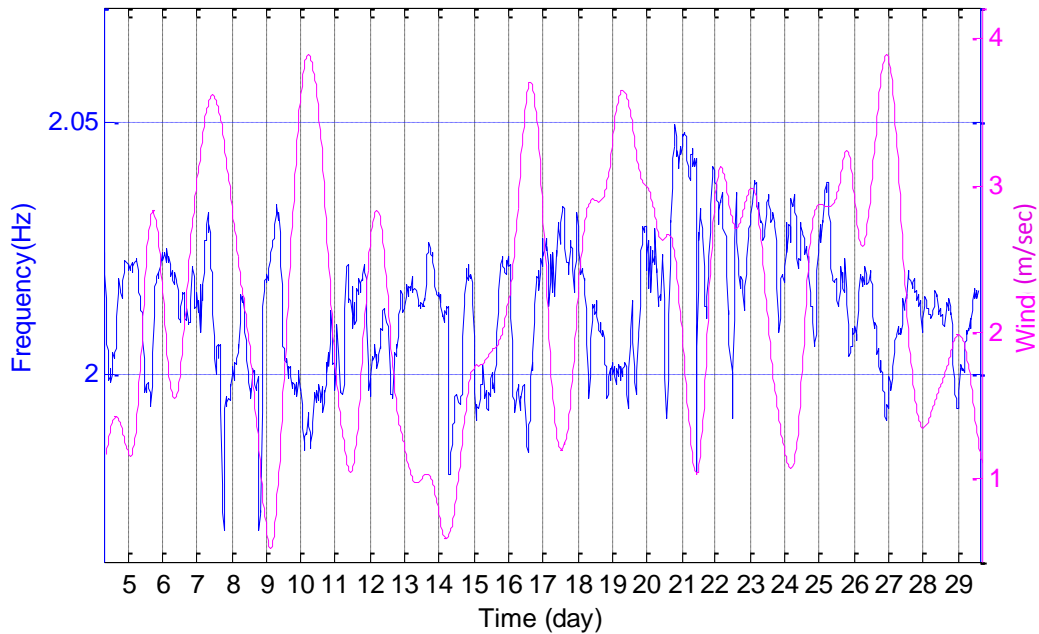


Figure 4.18. Variation of second modal frequency at station KUB1 and wind speed between 04.01.2013 and 30.01.2013 (in Y direction).

4.3. Precipitation

Precipitation is one of the factors supposed to affect vibration characteristics of structures. It has been shown that particularly in structures where soil-structure interaction plays a role on the dynamic response; precipitation tends to increase the natural period of vibration. The precipitation is related with humidity. Therefore, it needs to be assessed with humidity variation as well. The precipitation is a rapidly changing atmospheric event like wind speed. In this study, it is taken into account without considering the types of precipitation such as rain or snow. The main target is to observe whether rainfall or snowfall intensity have an impact on the modal properties of structures or not. In this context, the variation of precipitation amount per square meter is observed in one year and compared with frequency variation of the structure.

Results show that a significant relationship between precipitation and modal parameters is not observed in Hagia Sophia. Figure 4.19 and Figure 4.20 show annual

frequency variation with precipitation values at station KUB1 in X and Y directions respectively. In daily scale as well, there is not a remarkable effect. Figure 4.21 and Figure 4.23 show precipitation versus frequency variation in January 2013 for the first two directions. The period is chosen because of frequency (relatively less variation of frequency with temperature) and level of precipitation (higher compared to other months). In Figure 4.22 and Figure 4.24 we show frequency normalized by temperature versus precipitation for two periods in January and June. Normalization is done to remove the effect of temperature that is the most influential factor on ambient frequency. The two months are chosen as periods in order to observe pure precipitation effect. No correlation can be observed between frequency and precipitation levels.

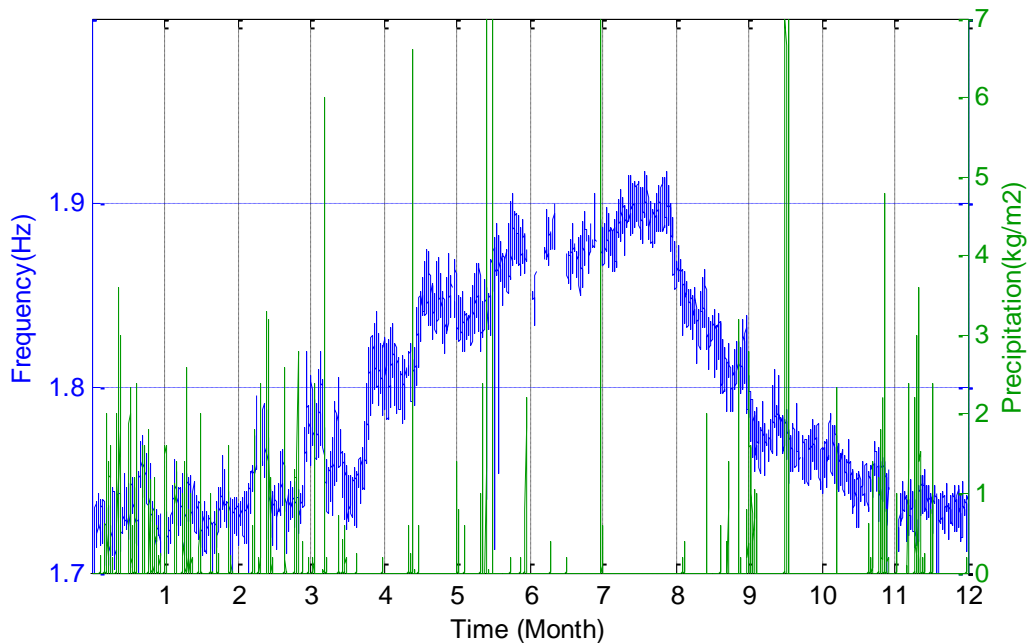


Figure 4.19. Variation of first modal frequency at station KUB1 and precipitation in year 2013 (in X direction).

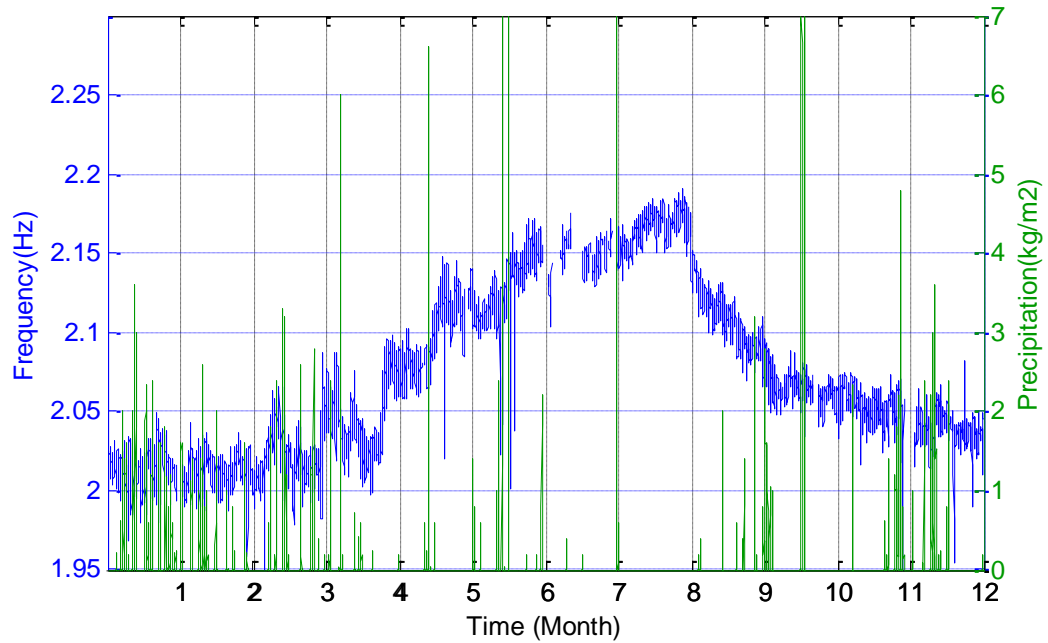


Figure 4.20. Variation of second modal frequency at station KUB1 and precipitation in year 2013 (in Y direction).

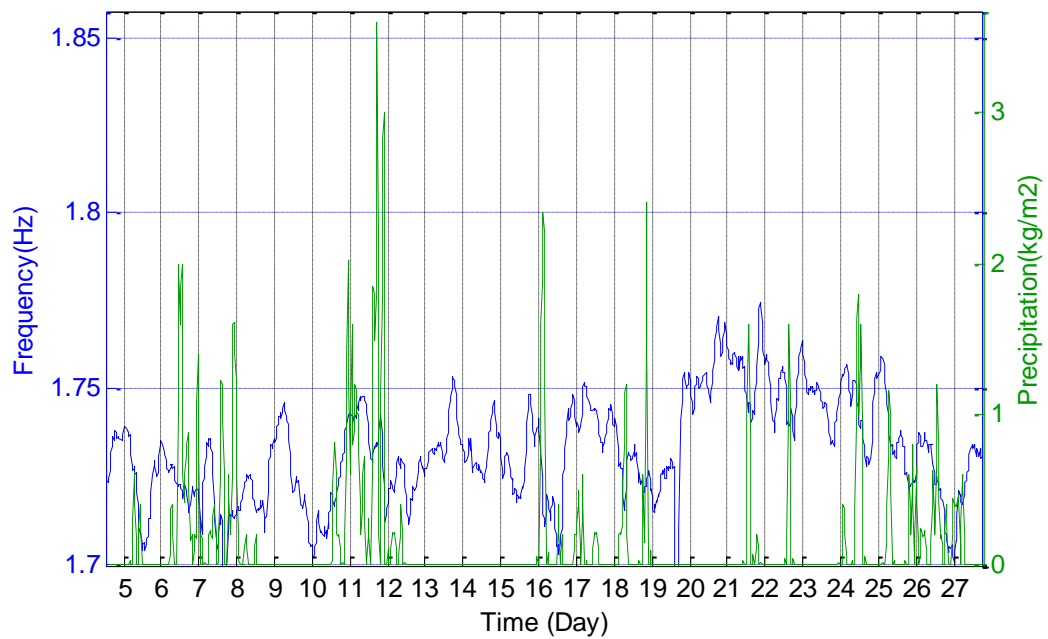


Figure 4.21. Variation of first modal frequency at station KUB1 and precipitation between 04.01.2013 and 28.01.2013 (in X direction).

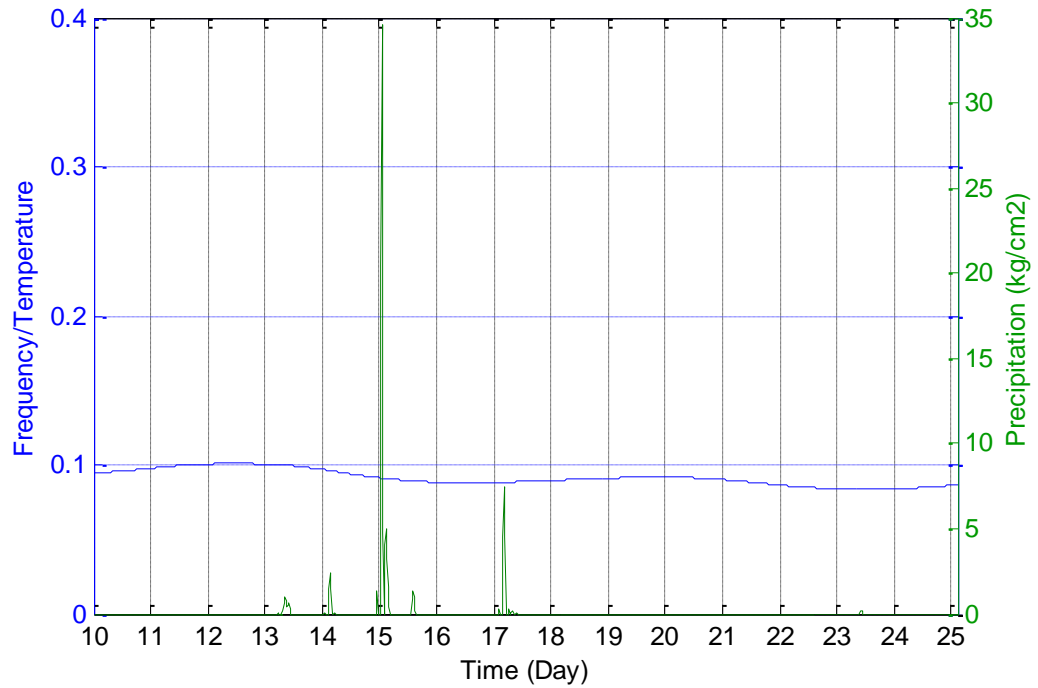


Figure 4.22. Variation of frequency/temperature ratio at station KUB1 and precipitation between 10.06.2013 and 25.06.2013 (in X direction).

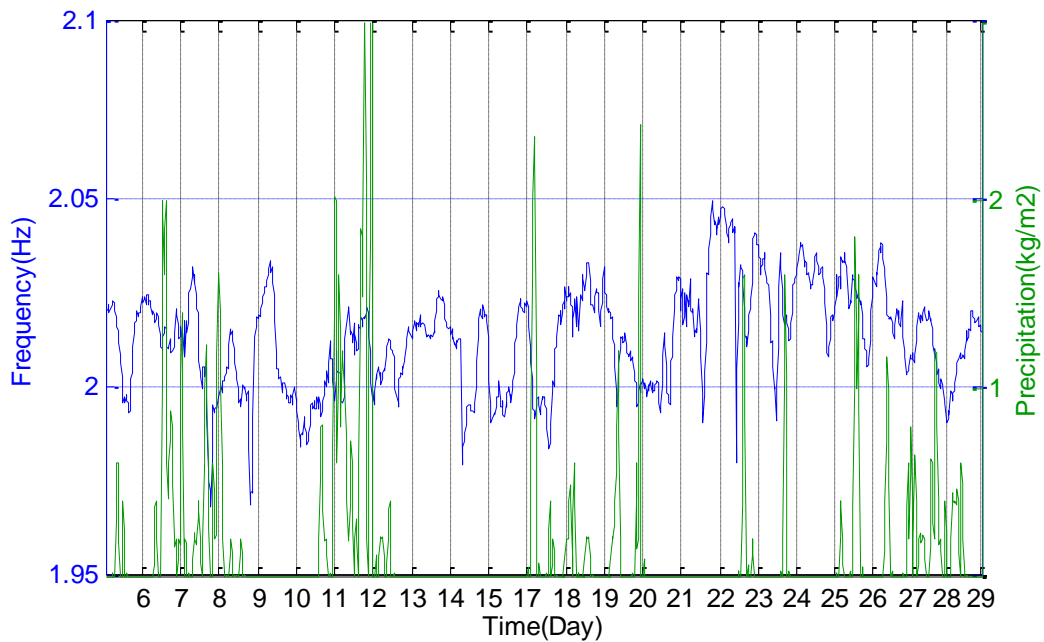


Figure 4.23. Variation of second modal frequency at station KUB1 and precipitation between 04.01.2013 and 28.01.2013 (in Y direction).

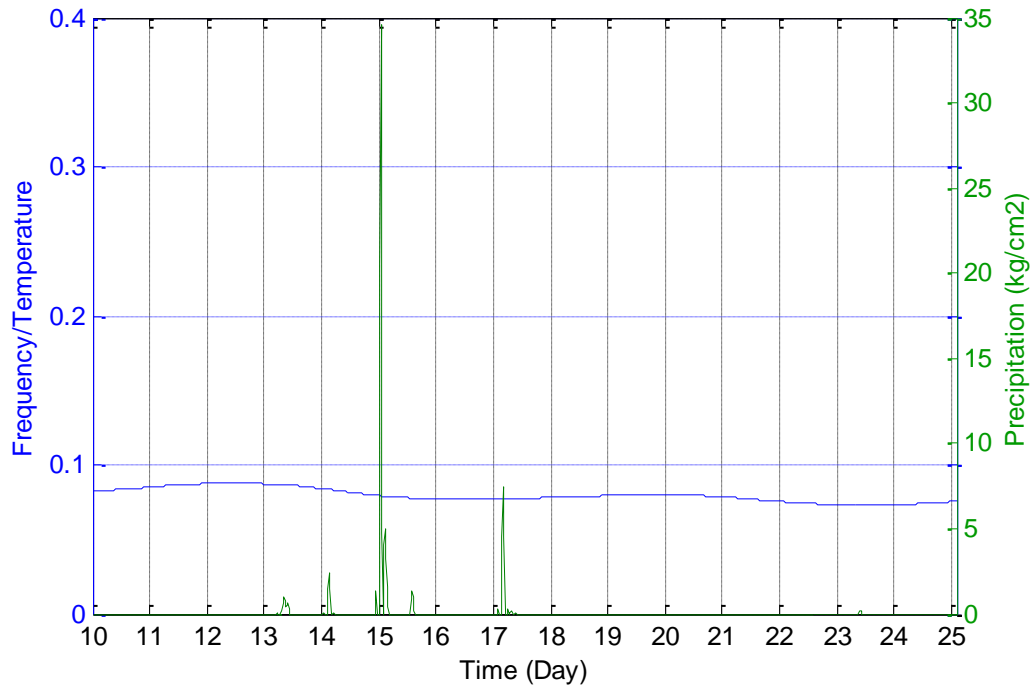


Figure 4.24. Variation of frequency/temperature ratio at station KUB1 and precipitation between 10.06.2013 and 25.06.2013 (in Y direction).

4.4. Humidity

The last atmospheric factor which may have significant effect on dynamic response parameters of Hagia Sophia is humidity. There are many types for humidity such as absolute humidity, relative humidity and specific humidity. In this study, relative humidity values are used to look for a relationship between humidity and ambient vibration.

Relative humidity can be expressed as the ratio of the current absolute humidity to the highest possible absolute humidity, which depends on the current air temperature. In other words, the relative humidity is the percent of saturation humidity. The moisture holding capacity of air decreases with drop in temperature while it increases with the rise in temperature. Therefore, relative humidity increases in winter and decreases in summer. Due to the fact that humidity is directly related with temperature, it is difficult to observe humidity effect on Hagia Sophia, as temperature is the dominant factor on its modal parameters. Figure 4.25 and Figure 4.27 show the annual relative humidity variation with modal

frequencies in X and Y directions respectively. The figures indicate that frequency of the structure increases while relative humidity decreases. However, this does not mean that humidity directly controls frequency variation. In fact, temperature variation dominantly controls both frequency variation and relative humidity, as shown in Figure 4.26 and Figure 4.28, where we co-plot frequency normalized by temperature and humidity for two modal frequencies.

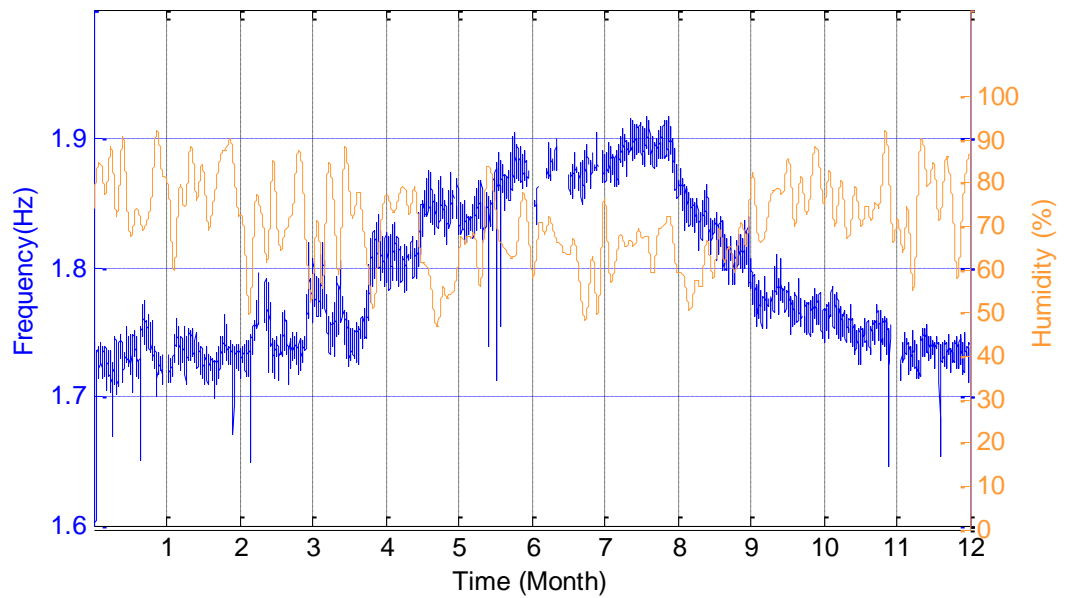


Figure 4.25. Variation of first modal frequency at station KUB1 and humidity in year 2013 (in X direction).

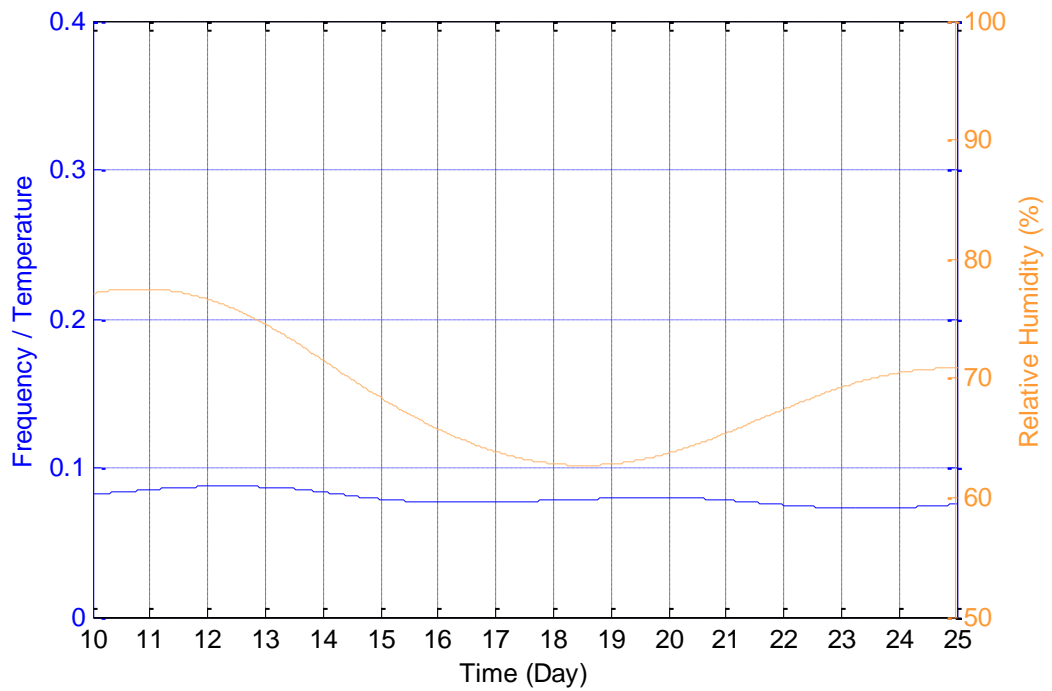


Figure 4.26. Variation of frequency/temperature ratio at station KUB1 and humidity between 10.06.2013 and 25.06.2013 (in X direction).

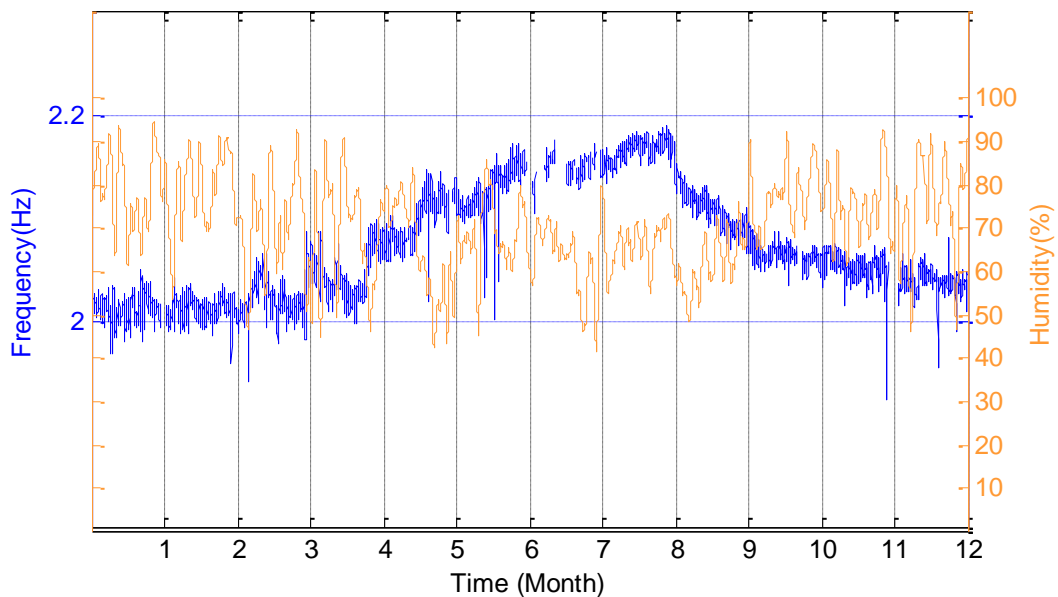


Figure 4.27. Variation of second modal frequency at station KUB1 and humidity in year 2013 (in Y direction).

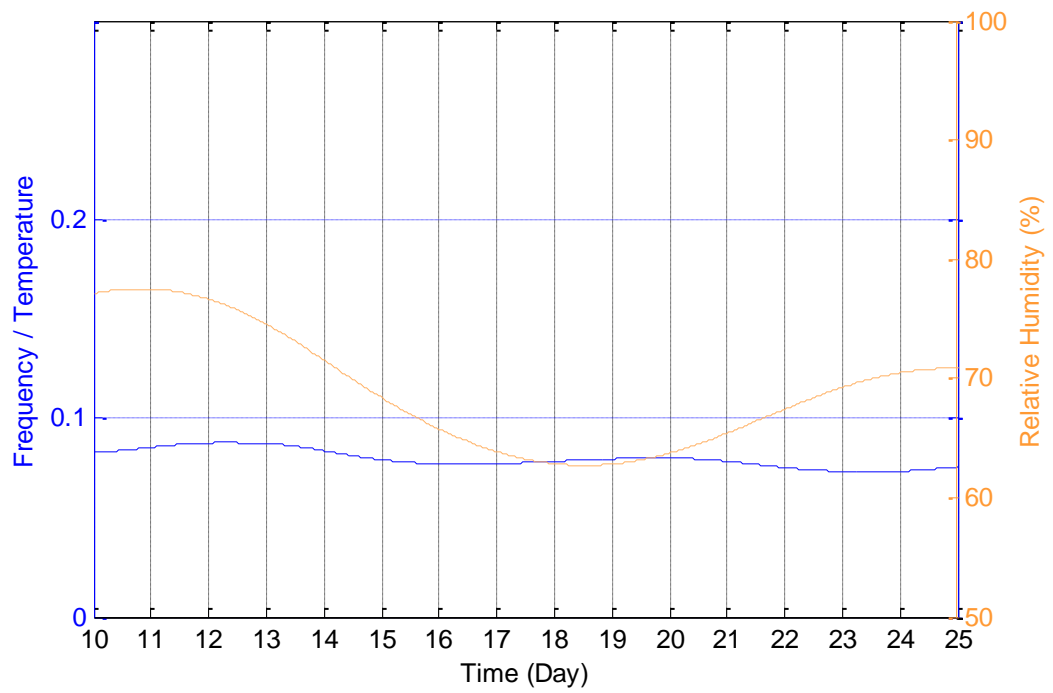


Figure 4.28. Variation of frequency/temperature ratio at station KUB1 and humidity between 10.06.2013 and 25.06.2013 (in Y direction).

5. ANALYSIS OF EARTHQUAKE RESPONSE

5.1. Time Domain Properties

Hagia Sophia experienced about a hundred earthquakes in the period between 2008 and 2014. Sixty-three of these earthquakes are analyzed and acceleration, velocity and displacement variations at all stations are calculated in three components. The peak values of acceleration, velocity and displacements at nine stations of Hagia Sophia are presented in Figure 5.1 through Figure 5.9.

The first notable fact after examination of records is the different magnitudes of accelerations between two directions. The maximum acceleration values recorded in the Y direction are always higher than those in the X direction.

Generally, it is expected that acceleration, velocity or displacement values recorded on structures are consistent with each other in plan and in section. Response of parts of structures with similar geometry and stiffness properties should be close to each other provided that they are undamaged. If there are no cracks or material problems on the bearing elements of the structure, structural elements need to behave in harmony with each other and transmission of accelerations from ground to upper floors should be at similar rates during earthquakes. However, most of the time this is not the case with masonry structures. In Hagia Sophia there are some inconsistencies at gallery and dome level with regard to acceleration transmission. We took into consideration many earthquakes in order to display this inconsistency.

In X direction, station KUB2 experiences acceleration values higher than those in other stations in all earthquakes (Figure 5.1), that are particularly larger than accelerations at station KUB4 located on the opposite side at the crown of the east main arch. To explain it with an example, during the M_L 6.5 Aegean Sea Earthquake that occurred on 24 May 2014

maximum acceleration recorded at station KUB2 was 22 cm/s^2 while the remaining dome level stations experienced accelerations about 11 cm/s^2 . This inconsistency is observed during all earthquakes measured at Hagia Sophia. The observation is valid for all peak velocities and displacements as well (Figure 5.4 and Figure 5.7). Station KUB2 is located at the crown of the west main arch. The stations at the top of the main piers where the west main arch springs from are GAL1 and GAL2.

In Y direction, a different problem is observed: stations GAL1, KUB1 and KUB2 measure higher acceleration values than their counterparts at the same level. To describe it with 24 May Aegean Sea Earthquake data, maximum acceleration values measured at GAL1, KUB1 and KUB2 stations are 20 cm/s^2 , 37 cm/s^2 and 24 cm/s^2 respectively while remaining six stations recorded accelerations in the range of $6\text{-}16 \text{ cm/s}^2$. Station KUB3 had very low acceleration values in Y direction in the time interval between December 2008 and November 2014 due to a technical problem. Therefore, the Y direction of KUB3 station is not taken into account in this evaluation. There is an excessive motion in the direction of Y at station GAL1 that corresponds to the southwest main pier, which is transmitted to stations KUB1 and KUB2 on the south and west main arches inducing relatively large accelerations in the same direction. As a result it can clearly be said that there is a problem associated with the southwest pier which was already noted by Durukal *et al.* (2003). The excessive vibrations in Y direction are transmitted to the south and west main arch, inducing in them higher amplitude accelerations, velocities and displacements, probably endangering their stability during a future large earthquake. This issue should be investigated thoroughly and carefully in the future by experimental and numerical studies.

In Z direction station KUB2 on the west main arch stands out. The level of vertical ground motion experienced at this station is comparable to horizontal level ground motions and are clearly higher than those experienced by the east main arch.

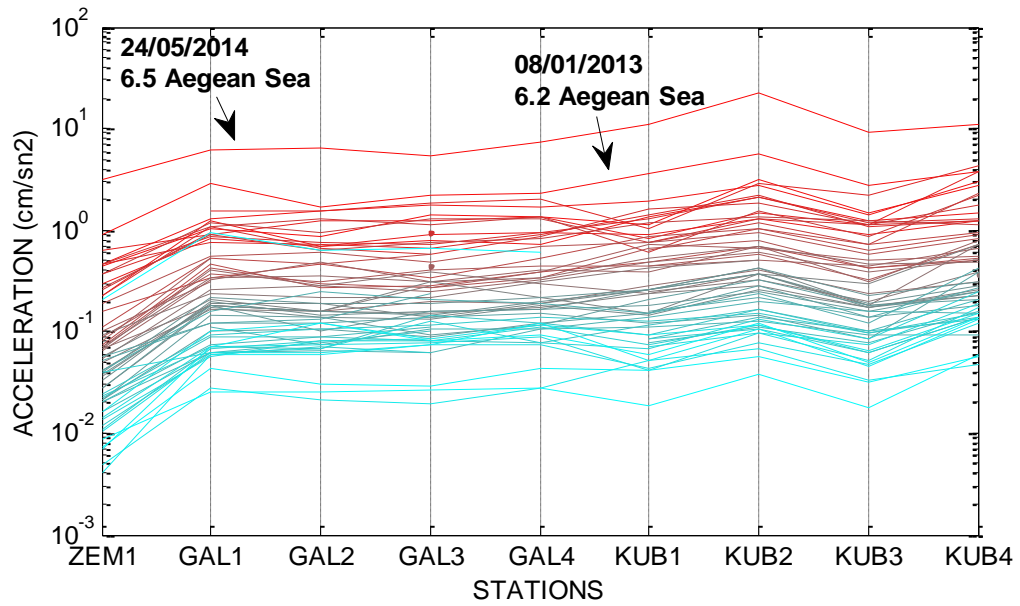


Figure 5.1. Peak horizontal (X) accelerations recorded at Hagia Sophia stations. Each line corresponds to an event. Two earthquakes that produced largest accelerations in Hagia Sophia are marked.

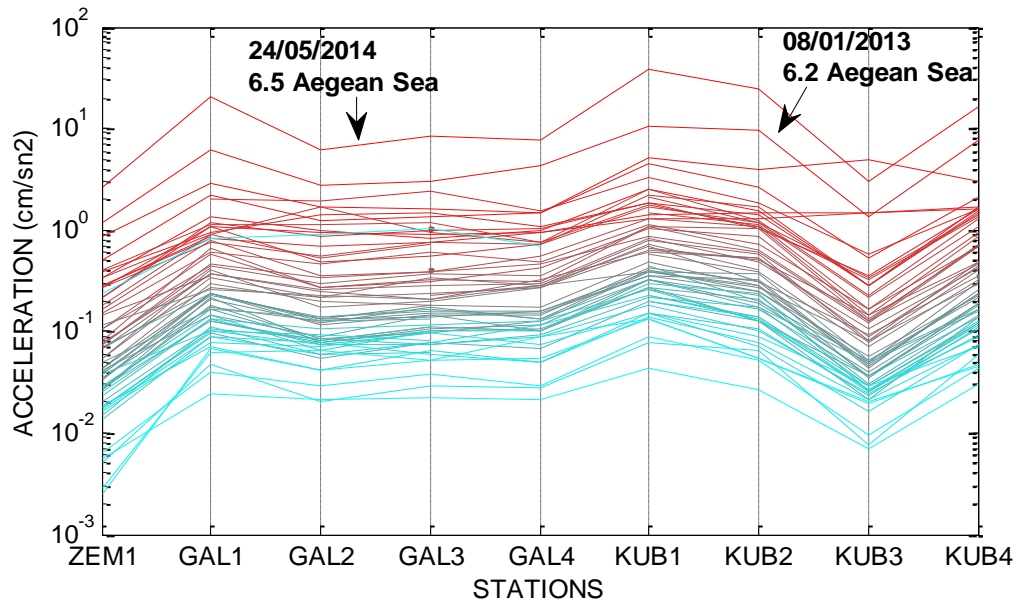


Figure 5.2. Peak horizontal (Y) accelerations recorded at Hagia Sophia stations. Each line corresponds to an event. Two earthquakes that produced largest accelerations in Hagia Sophia are marked.

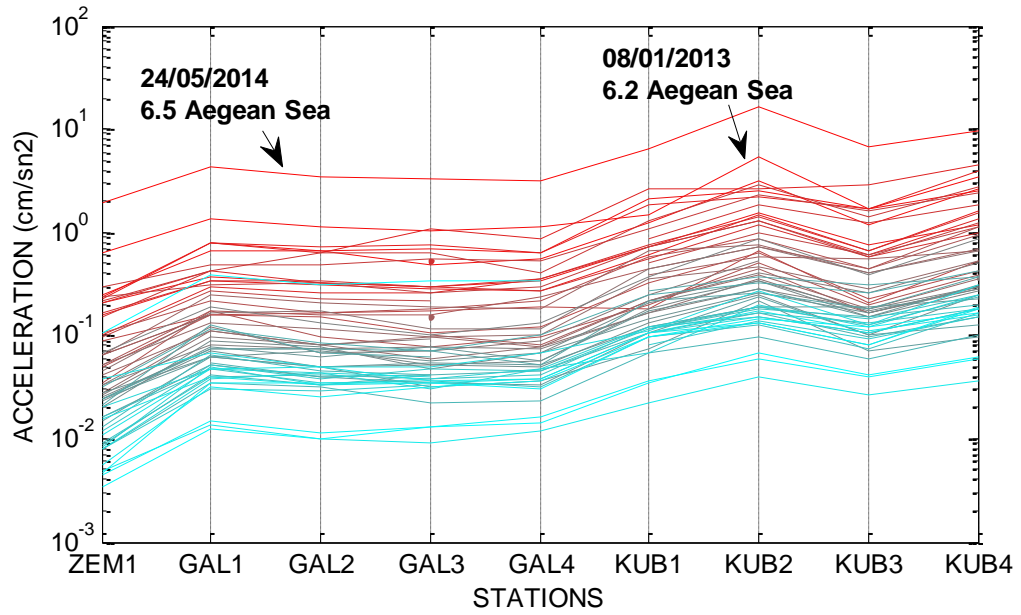


Figure 5.3. Peak vertical accelerations recorded at Hagia Sophia stations. Each line corresponds to an event. Two earthquakes that produced largest accelerations in Hagia Sophia are marked.

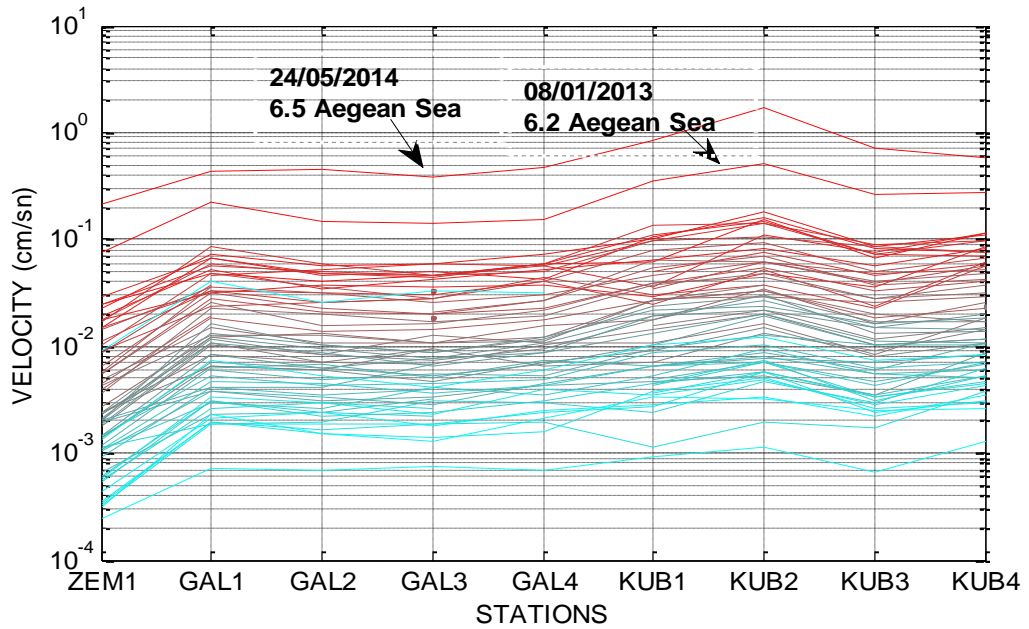


Figure 5.4. Peak horizontal (X) velocities at Hagia Sophia stations. Each line corresponds to an event. Two earthquakes that produced largest accelerations in Hagia Sophia are marked.

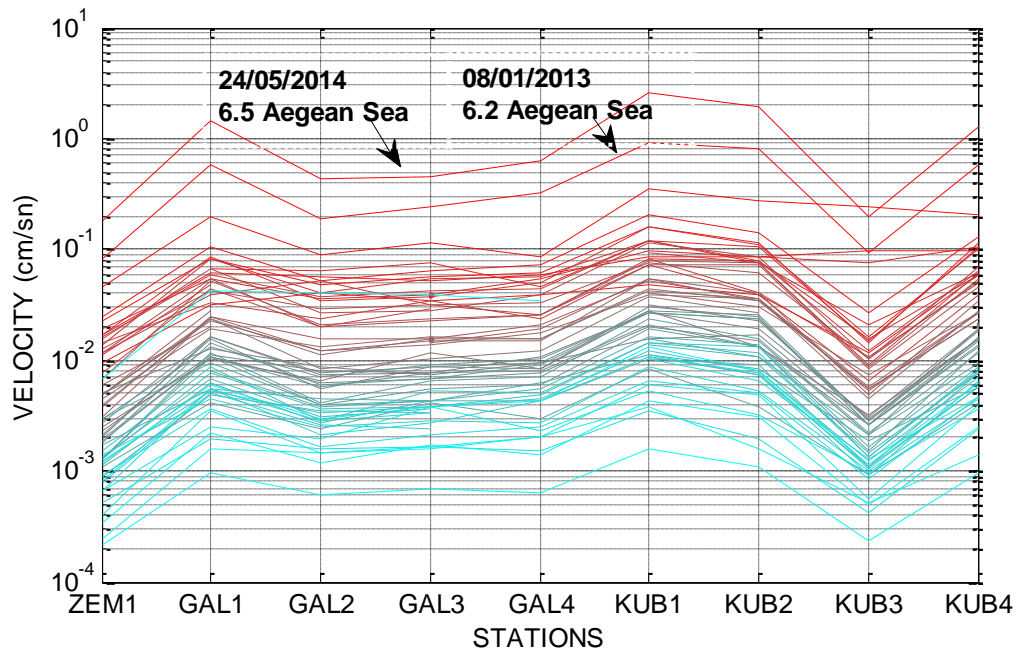


Figure 5.5. Peak horizontal (Y) velocities at Hagia Sophia stations. Each line corresponds to an event. Two earthquakes that produced largest accelerations in Hagia Sophia are marked.

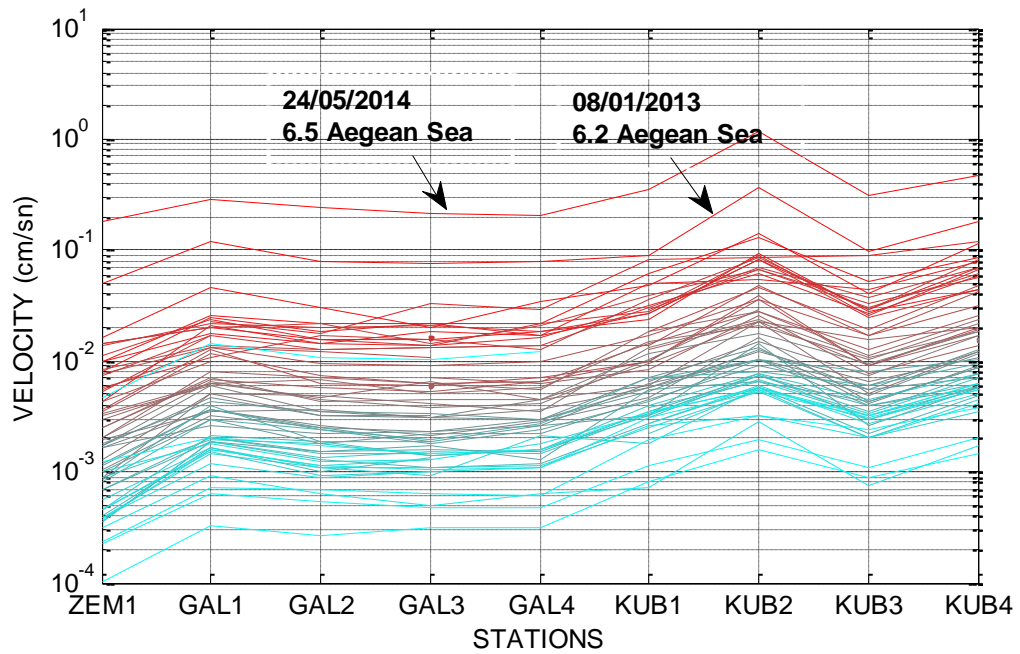


Figure 5.6. Peak vertical velocities at Hagia Sophia stations. Each line corresponds to an event. Two earthquakes that produced largest accelerations in Hagia Sophia are marked.

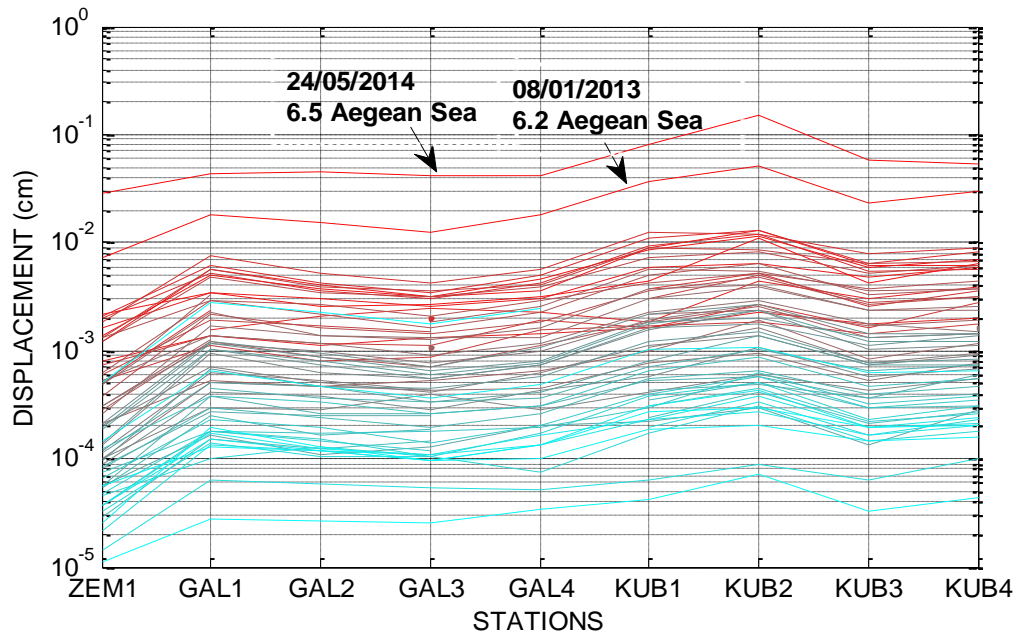


Figure 5.7. Peak horizontal (X) displacements at Hagia Sophia stations. Each line corresponds to an event. Two earthquakes that produced largest accelerations in Hagia Sophia are marked.

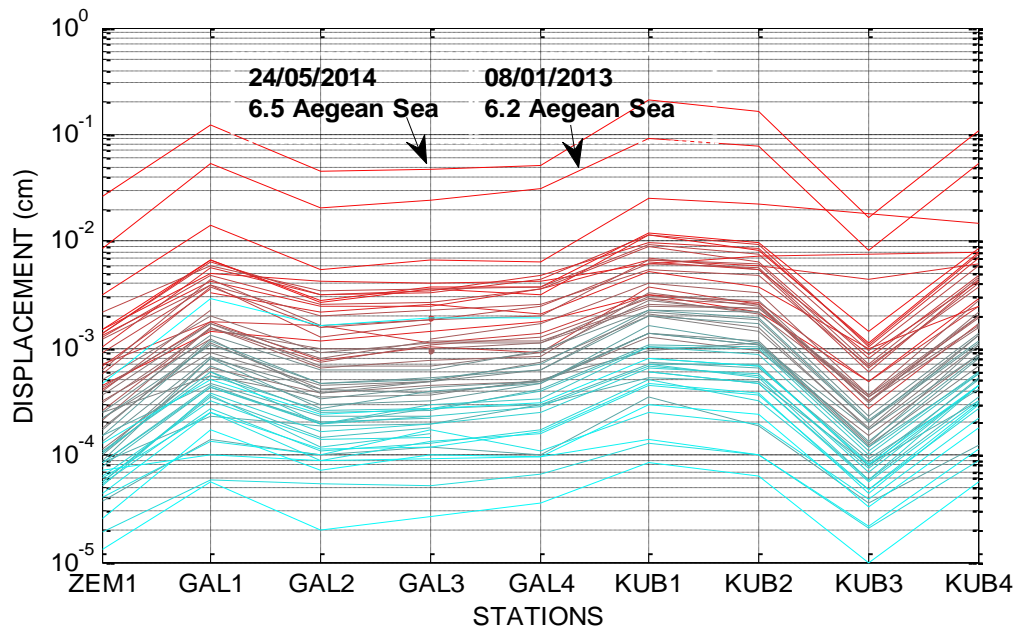


Figure 5.8. Peak horizontal (Y) displacements at Hagia Sophia stations. Each line corresponds to an event. Two earthquakes that produced largest accelerations in Hagia Sophia are marked.

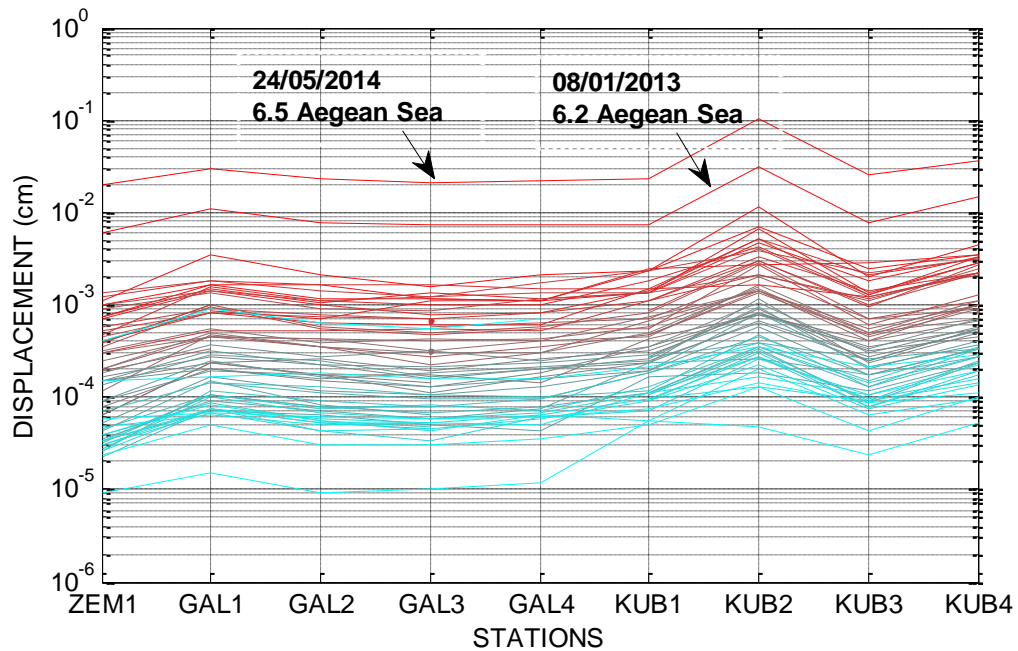


Figure 5.9. Peak vertical displacements at Hagia Sophia stations. Each line corresponds to an event. Two earthquakes that produced largest accelerations in Hagia Sophia are marked.

5.2. Frequency Domain Properties

Modal frequency is a significant parameter for monitoring modal properties and damage identification. The magnitude and location of damages can be correlated with the frequency variation before and after an earthquake. In this section, we determine the first two modal frequencies at Hagia Sophia stations. To this end, fifteen earthquakes having largest maximum accelerations at the ground station (ZEM1) in Hagia Sophia between the time interval 2008 and 2014 are selected for analysis. Earthquakes and identified frequencies are presented in Figure 5.10 and Figure 5.11.

Identified frequencies vary between 1.62 Hz and 1.82 Hz for the first mode and 1.75 Hz and 2.08 Hz in the second mode. It is observed that the lowest frequency corresponds to the 08.01.2013 Aegean Sea Earthquake, which produced second largest vibration amplitudes in the structure. The second lowest frequency corresponds to the 24.05.2014 Aegean Sea

Earthquake, which is the largest earthquake recorded at Hagia Sophia. As already noted before, the drop of frequency is not solely a function of earthquake magnitude or amplitude of experienced motion (Durukal *et al.*, 2003). We reiterate the same observation herewith as well. However the drop in frequency should be assessed with respect the pre-event frequency. Therefore the ambient vibration of the structure prior to earthquake needs to be considered to identify the frequency drop, as it has been shown that the frequency is directly related to temperature and wind speed at a particular time of the year. Due to the fact that the second largest earthquake occurred in winter, the frequency of the structure is lower than the frequency calculated in the largest earthquake.

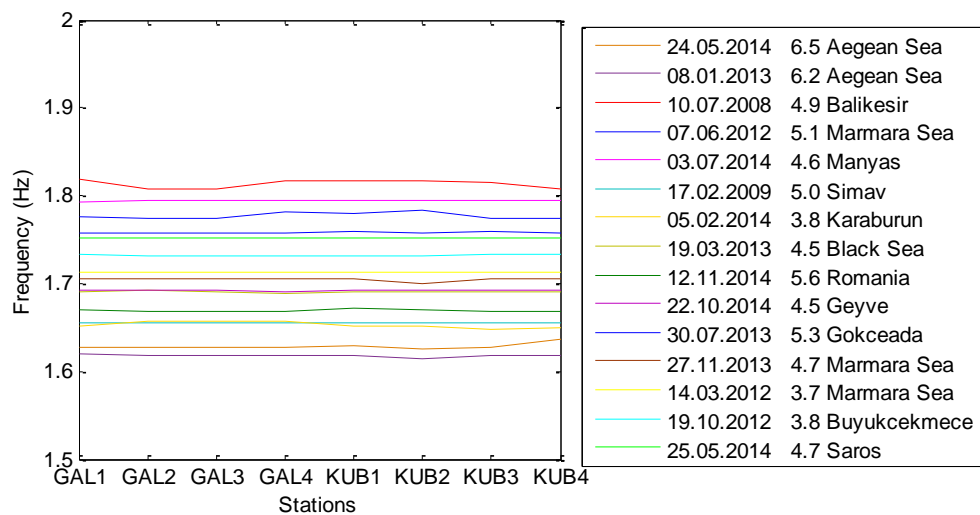


Figure 5.10. Identified first modal frequencies at Hagia Sophia stations during fifteen largest earthquakes that produced largest vibration amplitudes (X direction).

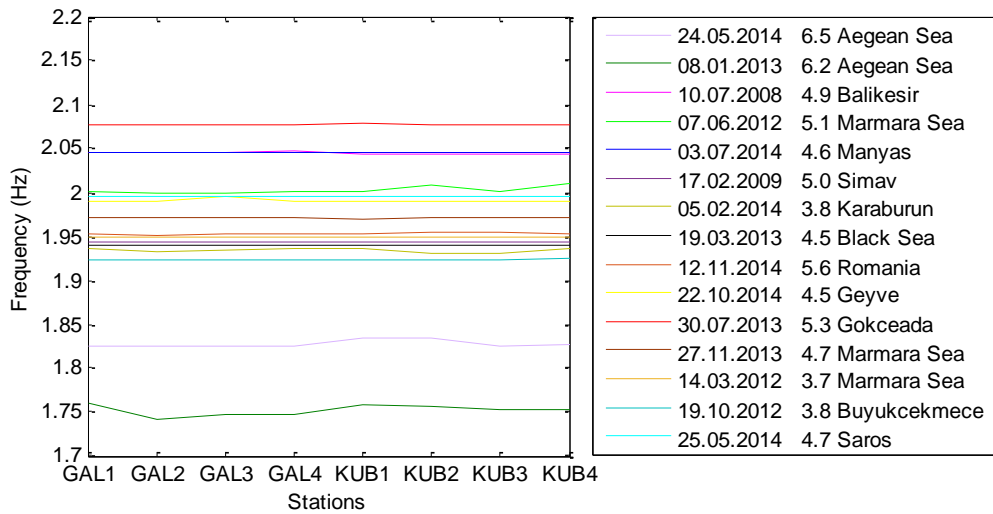


Figure 5.11. Identified second modal frequencies at Hagia Sophia stations during fifteen largest earthquakes that produced largest vibration amplitudes (Y direction).

The variation in modal parameters is not sufficient alone to develop an understanding about the dynamic behavior of structures. The Fourier amplitude spectra of acceleration at each station need to be analyzed. To comprehend the real behavior of Hagia Sophia, the Fourier amplitude spectrum of each station is estimated. An example is given from the 24 May 2014 Aegean Sea Earthquake. The records are band-pass filtered between 1.2 Hz and 2.5 Hz to constrain the range of interest for the first two modes. It is expected that the first mode dominates in X direction and the second mode is dominant in Y direction. The first two modes of the structure during 6.5 Aegean Sea Earthquake are in the range of 1.58-1.68 Hz and 1.78-1.88 Hz. However, it is revealed that the expected frequency ranges do not dominate at KUB2 station in X direction. The Fourier amplitude spectra at station KUB2 in two directions are shown in Figure 5.12 and Figure 5.13, which in fact demonstrate part of inconsistencies seen in the time domain. Contrary to expectations, the second mode prevails in the X direction at station KUB2 and leads to the diagonal motion in the first mode of KUB2. During the majority of the earthquakes, this spectral behavior is observed.

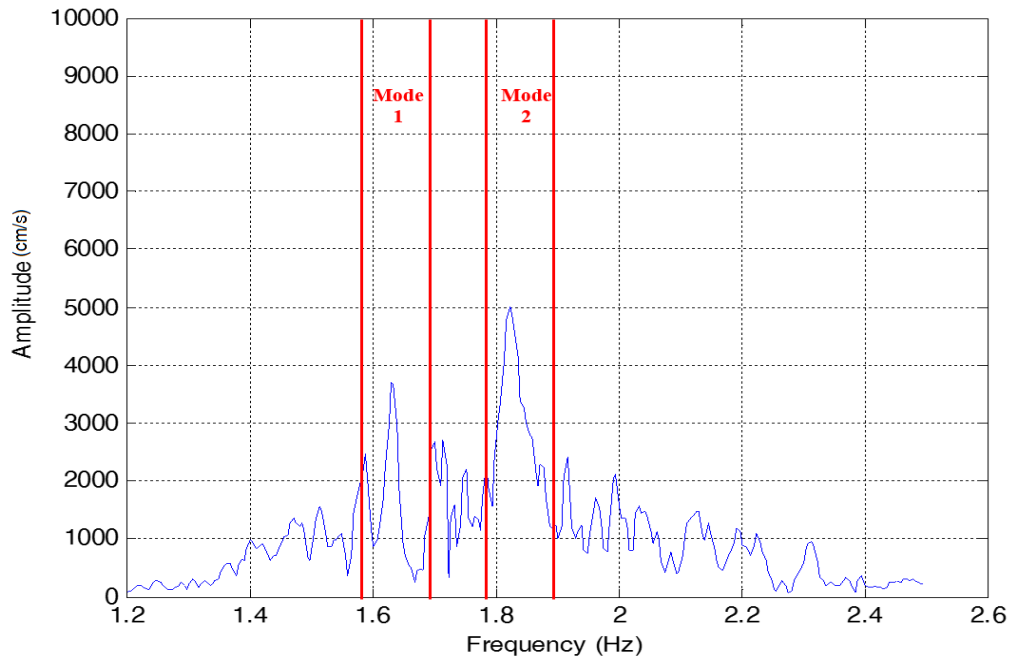


Figure 5.12. Fourier amplitude spectrum of station KUB2 during M6.5 Aegean Sea Earthquake in X direction.

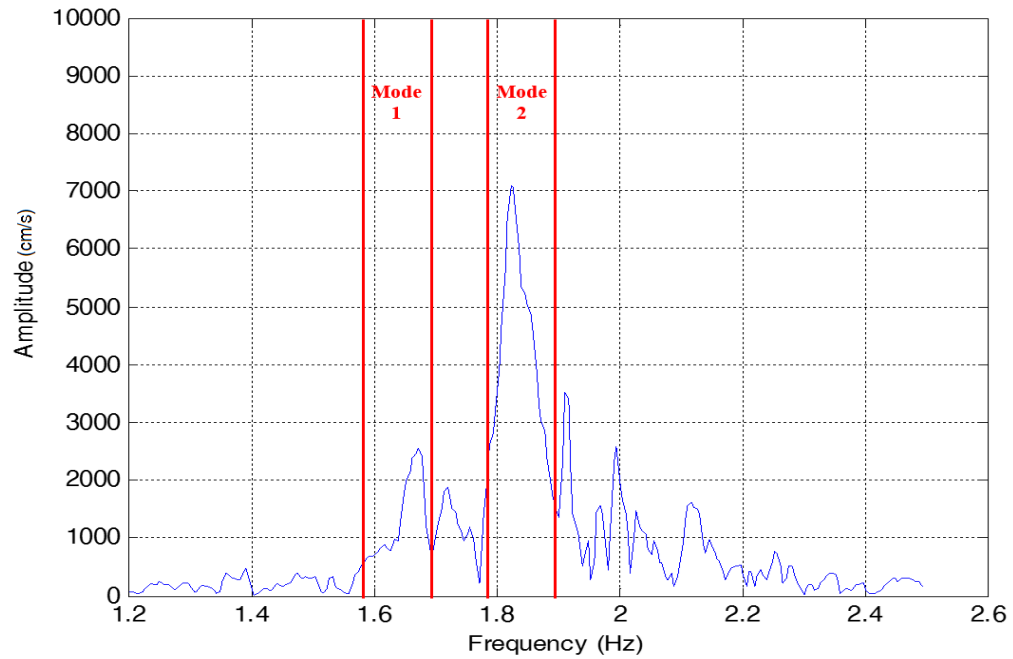


Figure 5.13. Fourier amplitude spectrum of station KUB2 during M6.5 Aegean Sea Earthquake in Y direction.

5.3. Mode Shapes

The mode shapes of historical buildings are expected to be more complex than modern structures due to the fact that they are associated with comparatively more irregular structural systems, inhomogeneous construction materials and past damages and repairs. Therefore, the mode shapes of historical buildings need to be assessed considering these special conditions.

Mode shapes can be calculated after the determination of modal frequencies in each earthquake. Supposing that all records are time-synchronized, mode shapes can be identified by examining the displacement time histories in two stages. Firstly, narrow-band-pass filtering is applied to acceleration records around each modal frequency. Secondly, modal displacements are obtained after double integrating the filtered acceleration. For this purpose, the earthquake inducing largest ground motion levels in Hagia Sophia (24.05.2014 Aegean Sea Earthquake) in our database is selected and the particle motions associated with the first two modes are presented in Figure 5.14 and Figure 5.15.

It appears that the first mode of the structure is not a pure lateral mode (Figure 48). Although the general sense of displacements is in the X direction, there is a very pronounced torsion involved. This result is different from the past studies performed on Hagia Sophia, in which the first mode was identified as dominantly lateral in X direction with some torsion. The second mode (Figure 5.15) is dominantly lateral and is not a mode purely in Y direction, as opposed to previous studies. Figure 5.14 and Figure 5.15 are drawn to the same scale for a better comparison of relative displacements across stations and modes. In order to look more closely at the details of particle motions associated with the first mode, they are estimated for three different earthquakes (Figure 5.16). It is seen that the dominant direction of motion is changing during earthquakes. When the P waves arrive, the motion starts on the X direction. With the arrival of S waves a 45° diagonal movement is induced, followed by displacements at about 90° to the previous ones. Displacements eventually die out mostly in the X direction. This sequence of changing directions during the earthquake is very similar in the three events studied (Figure 5.16). Thus what looks like torsion at the first look, is actually the building shifting between three dominant axes of vibration in the first mode. In

each case during the strong motion part (marked in red in Figure 5.16) and the following period where the amplitude of motion decreases, the sense of motion is dominantly in X direction. In the second mode, the motion starts, continues and ends dominantly in Y direction (Figure 5.17) with a similar display of displacements produced during the three events studied. Finally we need to point out that in both modes there is a distortion involved in the part of Hagia Sophia above the main piers, involving the main arches and the dome. This is evident from different angles of dominant sense of displacements between station GAL4 (gallery level) and KUB4 (dome level) (Figure 5.16 and Figure 5.17, left and right columns).

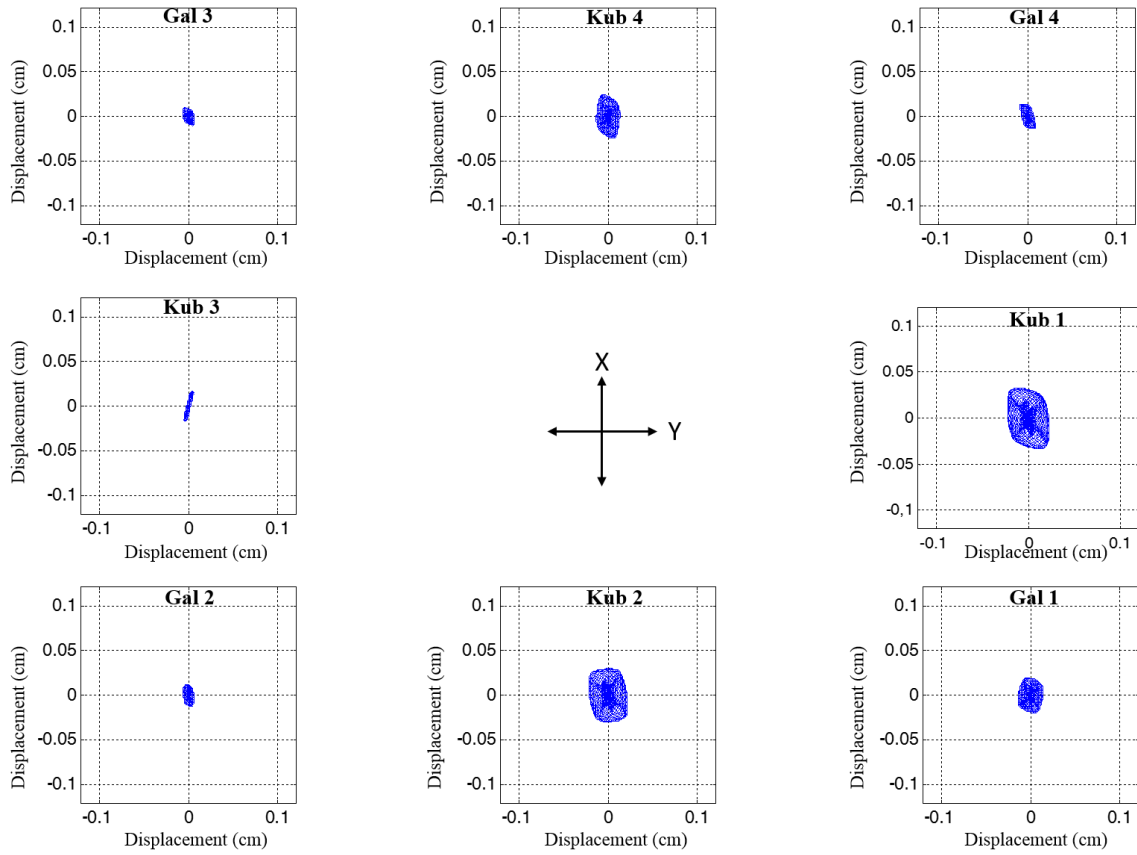


Figure 5.14. Particle motions corresponding to first modal frequency at Hagia Sophia stations during 6.5 Aegean Sea Earthquake (data filtered between 1.58 and 1.68 Hz).

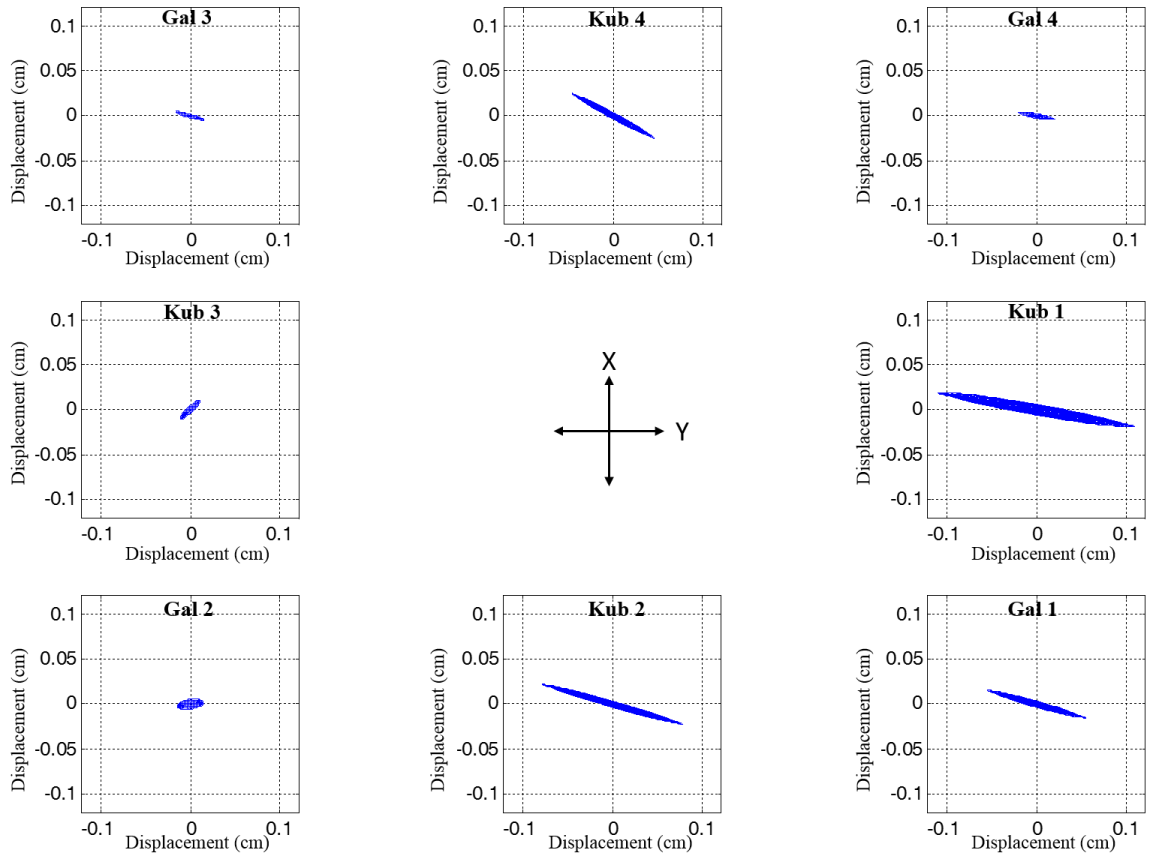


Figure 5.15. Particle motions corresponding to second modal frequency at Hagia Sophia stations during 6.5 Aegean Sea Earthquake (data filtered between 1.78 and 1.88 Hz).

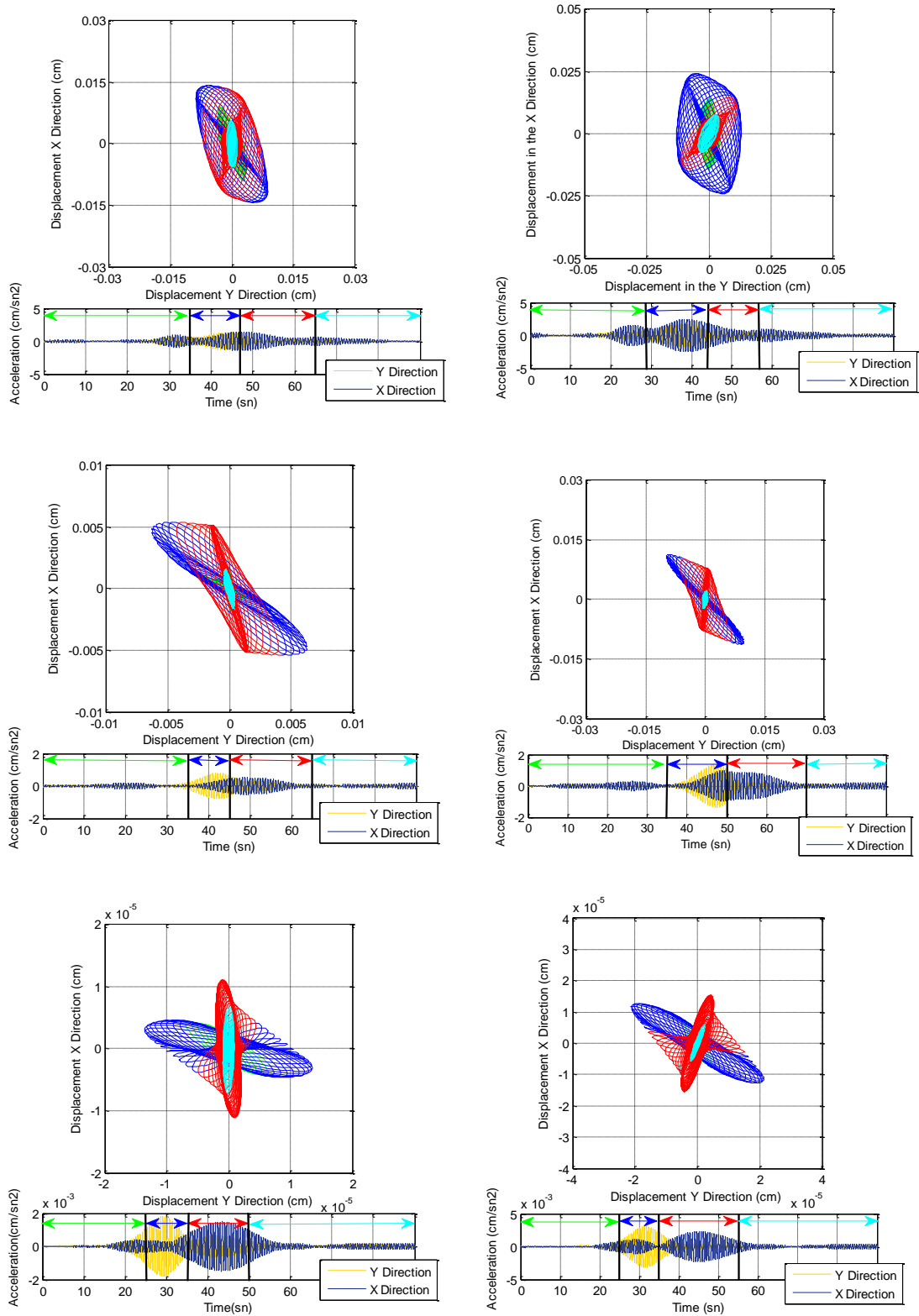


Figure 5.16. Particle motions corresponding to first modal frequency at stations GAL4 (left column) and KUB4 (right column) during three earthquakes: 6.5 Aegean Sea 2014, (top row), 6.2 Aegean Sea 2013 (middle row), 4.9 Balıkesir 2008 (bottom row).

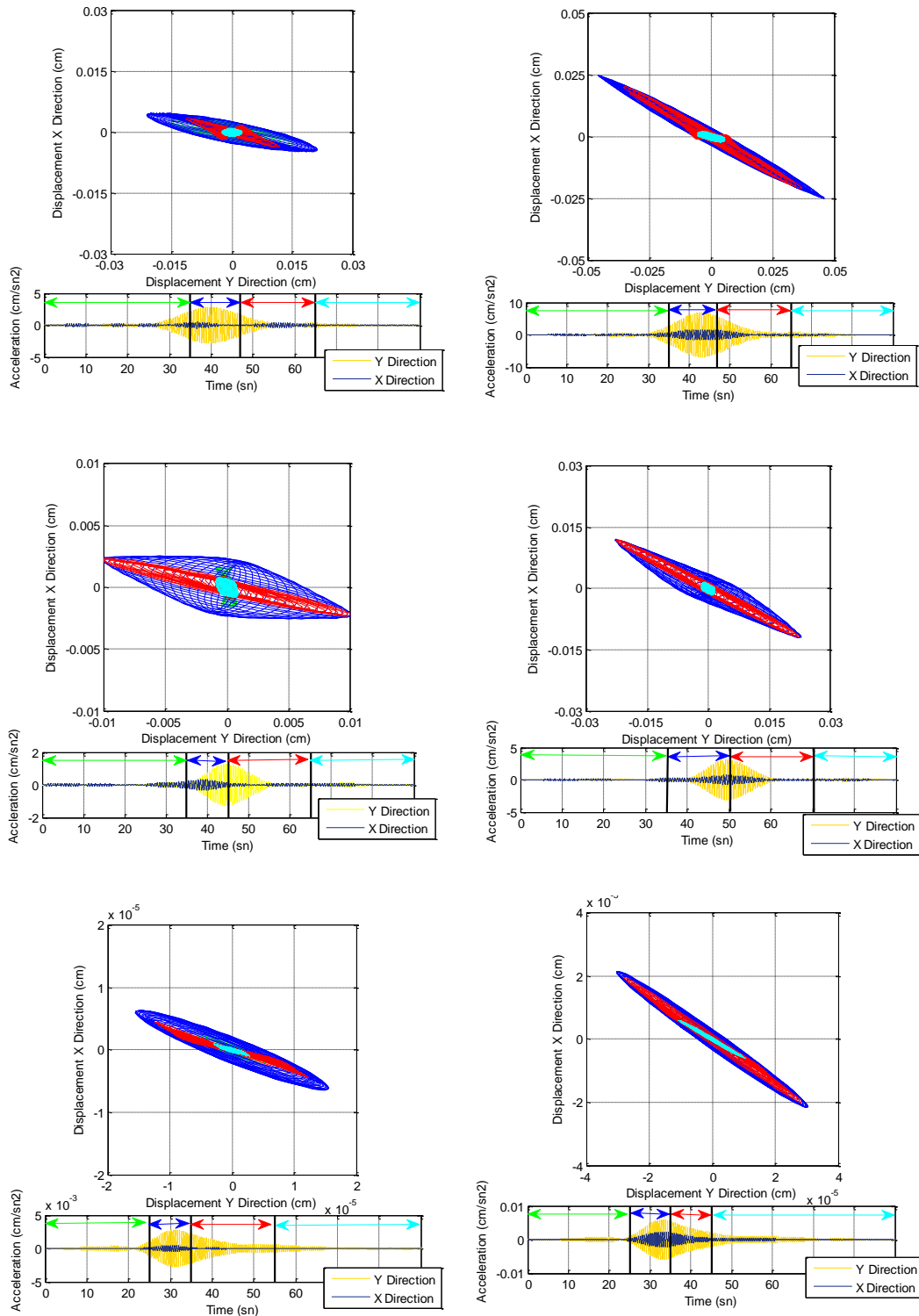


Figure 5.17. Particle motions corresponding to second modal frequency at stations GAL4 (left column) and KUB4 (right column) during three earthquakes: 6.5 Aegean Sea 2014,(top row), 6.2 Aegean Sea 2013 (middle row), 4.9 Balıkesir 2008 (bottom row).

5.4. Variation of Modal Frequencies with Vibration Amplitude and Duration

Duration and vibration amplitude of earthquakes are two parameters that are supposed to have an impact on frequency drop of structures. To see the impact of duration and maximum acceleration on Hagia Sophia, first, the frequency drop (ΔF) is evaluated in X and Y directions. The frequency drop is calculated by subtracting the frequency value estimated prior to earthquake excitation from frequency value during excitation. Normalization is done with respect to pre-event frequency. To represent the whole structure the drop representing an event is calculated as the average of station-based drop values.

Secondly, the duration of strong ground motion part of recordings of largest fifteen earthquakes are calculated. The duration varies depending on earthquake magnitude and local site response. Generally, long duration strong motion is expected to be more hazardous for structures. Therefore, duration is a significant parameter with respect to the quantification of damage potential of earthquake ground motion.

Significant duration can be described as the time interval between the points at which 5% and 95% of total energy has been recorded. Arias intensity can be identified as accumulation of energy in the strong ground motion. Our studies show that the points at which 5% and 95% of total energy cannot identify duration accurately if the measured acceleration is too small. Therefore, for small ground motions, starting threshold values of significant durations are selected as the points at 10% or 15% of total energy while end threshold values of significant durations are selected as the points corresponding to 90% or 85% of total energy respectively in this study. Figure 5.18 shows frequency drop versus significant duration in X and Y directions. It is evident from Figure 5.18 that no direct relationship exists between significant duration of strong ground motion and frequency drop of the structure. This probably necessitates a better definition for characterization of duration at low amplitude ground motion. The duration of the S-wave part will probably yield a better correlation.

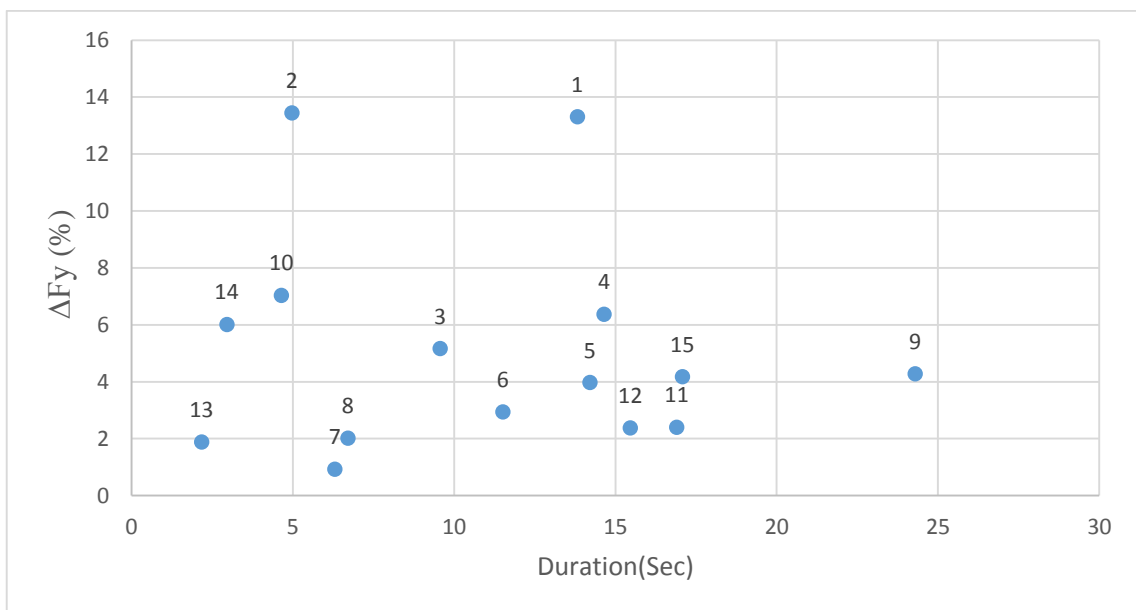
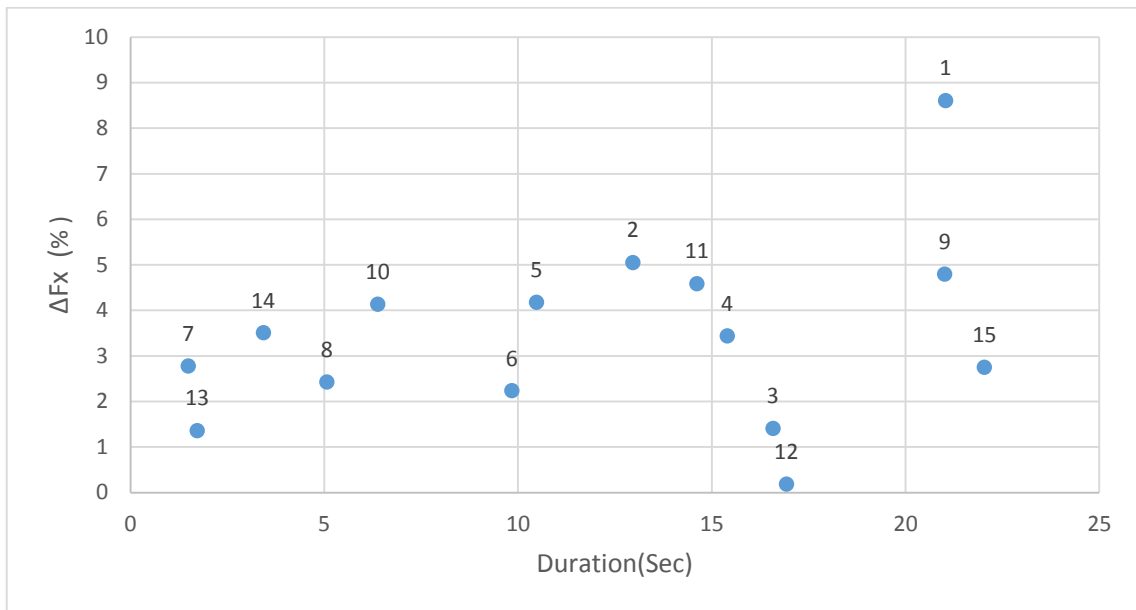


Figure 5.18 . Drop in first (top) and second (bottom) modal frequencies with respect to duration.

Thirdly, the peak accelerations of fifteen earthquakes are calculated. Figure 5.19 shows the relationship between peak acceleration and frequency drop. The figure indicates a direct relationship between frequency drop of the structure and maximum acceleration of

ground motion that probably will be enhanced when more recordings with higher amplitudes are obtained in Hagia Sophia.

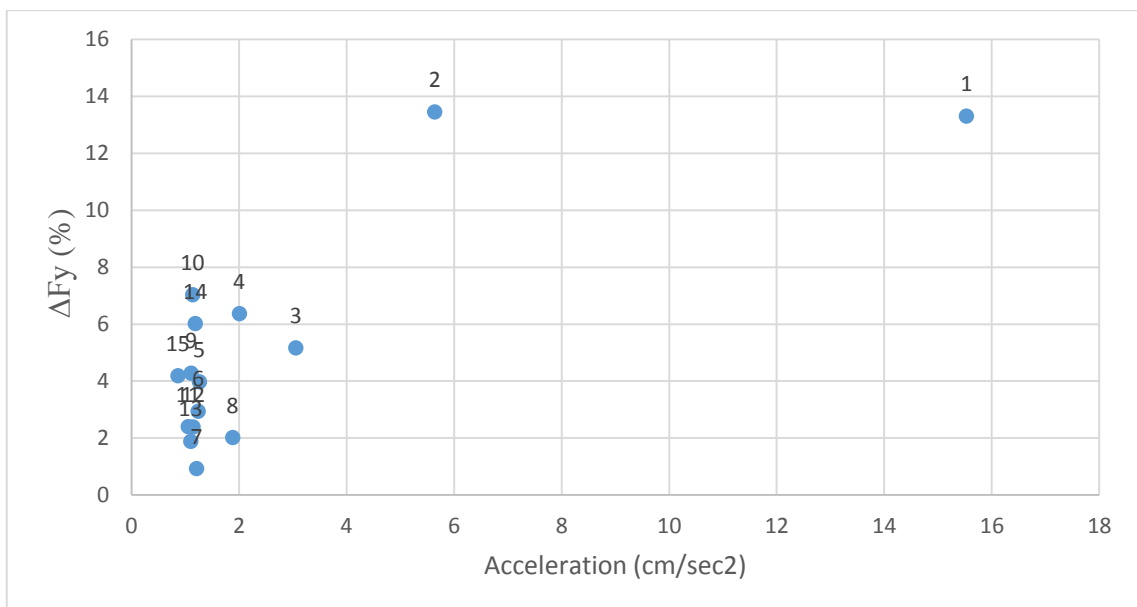
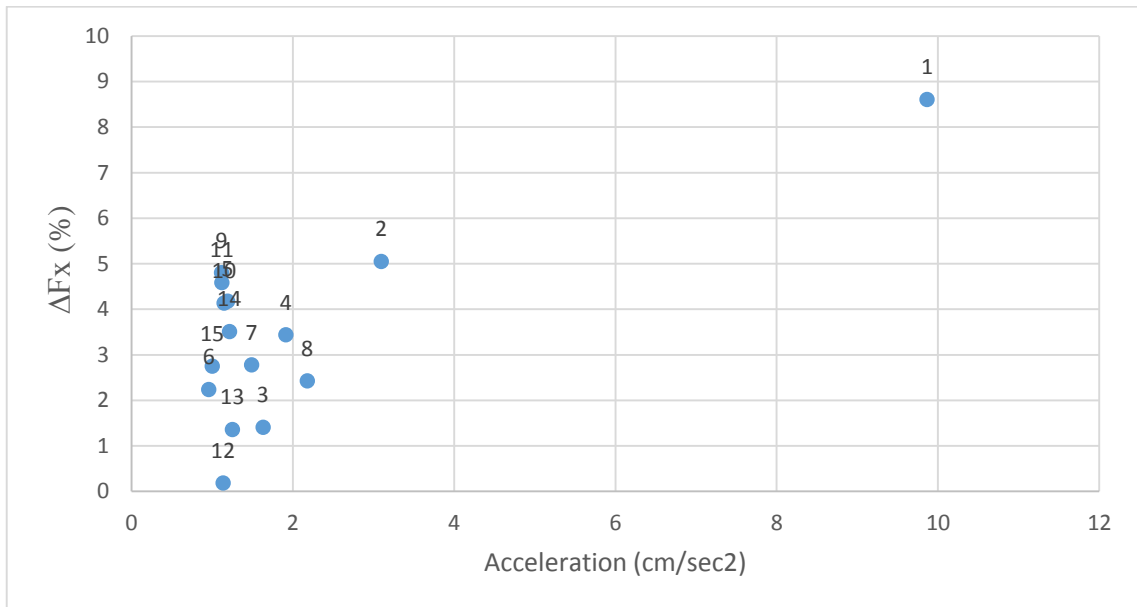


Figure 5.19. Drop in first (top) and second (bottom) modal frequencies with respect to peak acceleration at the ground level of Hagia Sophia.

6. CONCLUSIONS

The influence of external sources on structural vibration characteristics is a significant issue not only for the protection of heritage buildings but also for general civil engineering practice. The identification and assessment of external sources ensure keeping the structural vibration levels under control. In this study, uncertainties induced by environmental effects such as temperature change, wind speed, precipitation and humidity are examined and their effects on modal frequencies and damping properties of Hagia Sophia are investigated.

The results show that temperature change is directly related with the variation of modal frequencies of Hagia Sophia. The first modal frequencies in two orthogonal directions increase with the rise of temperature in the transition from winter to summer and decrease with the temperature towards winter months. The increase in frequency is 9.8% for the first mode and 7.4% for the second mode. It is found that modal frequencies are not only sensitive to long-term temperature variations across the seasons, but also to temperature changes within a month and even within one day.

Although subtle, wind has influence on the vibration properties of the structure. It was observed that with increased wind speeds the modal frequencies tend to drop. The observation is clear at times when the temperature change does not dominate the variation in frequency.

No significant correlation between precipitation, humidity and structural vibration characteristics of Hagia Sophia is observed.

The decrease in modal frequencies of Hagia Sophia is directly proportional to vibration amplitudes. It should also be correlated with the duration of strong ground motion. With the definition used for strong motion duration in this study, this correlation could however not be shown. It is believed a better definition will perform better.

Based on analysis of earthquake data recorded between 2008 and 2014 in Hagia Sophia, maximum drop in the first modal frequency is estimated as 9%. In the second modal frequency it is 14%. It should be noted that these drops are very close to the frequency variations induced by temperature changes, to which Hagia Sophia has been exposed to for about 1500 years.

There are structural elements in Hagia Sophia, which need detailed in-situ investigations in search of possible deficiencies. They are the southwest main pier, the west main arch and the south main arch. Southwest main pier stands out with its excessive vibration amplitudes in Y direction, west main arch displays comparatively higher amplitude motions in particularly X and Z directions and the south main arch experience significant levels of accelerations in Y direction.

Modal shapes of Hagia Sophia are not pure, but complex. Particle motions obtained by narrow-band-pass filtering displacements indicate that the first modal shape is dominantly in X-direction, while the second mode shape is in Y direction, with a component in X direction. In both modes there is a distortion in the clock wise direction with respect to the sense of motion of the main piers, involving the main arches and the dome.

REFERENCES

- Aktan, AE, F.N. Catbas., K.A. Grimmelsman and C.J. Tsikos, 2000, "Issues in Infrastructure Health Monitoring for Management" *Journal of Engineering Mechanics (ASCE)*, Vol. 126, pp. 711–724.
- Alampalli, S., 1998, "Influence of In-service Environment on Modal Parameters", *Proceedings of the 16th International Modal Analysis Conference (IMAC-XVI)*, Santa Barbara, California.
- Almac, U., K. Schweizerhof , G. Blankenhorn, C. Duppel and F. Wenzel, 2013, "Structural Behaviour of Hagia Sophia Under Dynamic Loads" *Vienna Congress on Recent Advances in Earthquake Engineering and Structural Dynamics*, Vienna, Austria, pp. 475.
- Arias, A., 1970, "A Measure of Earthquake Intensity" R.J. Hansen, ed. *Seismic Design for Nuclear Power Plants*, MIT Press, Cambridge, Massachusetts, pp. 438-483.
- Aoki, T., S. Kato and K. Ishikawa, 1993, "Structural Characteristics of the Dome of Hagia Sophia from Measurement of Micro Tremor" *Computational Mechanics Publications*, Southampton, United Kingdom, pp. 115-122.
- Aoki, T., S. Kato, K. Ishikawa, K. Hidaka, M. Yorulmaz and F.Çili, 1997, "Principle of Structural Restoration for Hagia Sophia Dome", *Proceedings of STREMAH International Symposium*, pp. 467-476.
- Carden, E. P and P. Fanning, 2004, "Vibration Based Condition Monitoring: A Review", *Structural Health Monitoring* pp. 3- 355.

- Chang, P. C., C. A. Flatau and S. C. Liu, 2003, "Review Paper: Health Monitoring of Civil Infrastructure" *Structural Health Monitoring*, pp. 2- 257.
- Clinton, F. John, 2004, *Modern Digital Seismology - Instrumentation, and Small Amplitude Studies in the Engineering World*, Ph.D Thesis, California Institute of Technology.
- Çakmak, A.Ş., C.L. Mullen and M.Erdik, 1992, *Measured Nonlinear Response of the Hagia Sophia Masonry Structure to a Low-Level Earthquake*, Research Report, Princeton University.
- Çakmak, A.Ş., R. Davidson, C. Mullen and M. Erdik, 1993, "Dynamic Analysis and Earthquake Response of Hagia Sophia", *Structural Repair and Maintenance of Historical Buildings III*, Proceedings of the third International Conference held at Bath in June 1993, edited by C.A Brebbia and R.J.B. Frewer, Southampton, pp. 67-84.
- Çakmak, A.Ş., A. Moropoulou and C. L. Mullen, 1995, "Interdisciplinary Study of Dynamic Behavior and Earthquake Response of Hagia Sophia", *Soil Dynamics and Earthquake Engineering*, pp. 125-133.
- Çaktı, E., 1992, *A Study on Structural Identification and Seismic Vulnerability Assessment of Aya Sofya*, M.Sc. Thesis, Boğaziçi University.
- Davenport, A.G., 1961, "The Application of Statistical Concepts to the Wind Loading of Structures," *Proceedings of Institution of Civil Engineers*, Vol. 71, pp. 19-449.
- Davidson, R. A., 1993, *The Mother of All Churches: A Static and Dynamic Structural Analysis of Hagia Sophia*, Senior Thesis, Princeton University.

- Dunnicliff, J., 1993, *Geotechnical Instrumentation for Monitoring Field Performance*, Wiley-IEEE, New York, NY, USA.
- Durukal, E., S. Cimilli and M. Erdik, 2003, “Dynamic Response of Two Historical Monuments in Istanbul Deduced from the Recordings of Kocaeli and Düzce Earthquakes” *Bulletin of the Seismological Society of America*, Vol. 93, No. 2, pp. 694–712.
- Erdik, M. and E. Durukal, 1993, “Protection of Architectural Heritage against Earthquakes”, *Ministry of Public Works and Settlement*, pp.37-47, Ankara.
- Erdik, M., E. Durukal, G. Yüzügüllü, K. Beyen and U. Kadakal, 1993, “Strong-motion Instrumentation of Aya Sofya and the Analysis of Response to an Earthquake of 4.8 Magnitude.” *Soil Dynamics and Earthquake Engineering VI, Computational Mechanics Publications, Southampton, co-published with Elsevier Applied Science*, London, New York, pp. 899-914.
- Gueguen, P., M. Langlais, P. Roux, J. Schinkmann and I. Douste-Bacqué, 2014, “Frequency and Damping Wandering in Existing Buildings Using the Random Decrement Technique”, *7th European Workshop on Structural Health Monitoring*, Nantes, France
- Holmes, J.D., 2001, *Wind Loading of Structures*, Spon Press, Oxford, UK.
- Jinping, O. and H. Li, 2010, “Structural Health Monitoring in Mainland China: Review and Future Trends” *Structural Health Monitoring*, Vol. 9, No. 3, pp. 9-219.
- Kaya, Y., 2009, *Tools and Techniques for Real-Time Modal Identification*, Ph.D. Thesis, Boğaziçi University.

- Kırlangıç, A.S., 2008, *Re-Evaluation of Earthquake Performance and Strengthening Alternatives of Hagia Sophia*, M.Sc. Thesis, Boğaziçi University.
- Ko, J.M. and Y.Q. Ni, 2005, “Technology Developments in Structural Health Monitoring of Large-scale bridges” *Engineering Structures*, Vol. 27, pp. 1715–1725.
- Mainstone and Rowland J., 1998, *Hagia Sophia: Architecture, Structure and Liturgy of Justinian's Great Church*. Thames & Hudson, London, UK.
- Mark, R., A.S. Çakmak, K. Hill and R. Davidson, 1993, “Structural Analysis of Hagia Sophia: A Historical Perspective” *In: Proceedings of the soil dynamics and earthquake engineering VI*, pp. 867-880.
- Martins N., E. Caetano, S. Diord, F. Magalhães and A. Cunha, 2014, “Dynamic Monitoring of a Stadium Suspension Roof: Wind and Temperature Influence on Modal Parameters and Structural Response”, *Engineering Structures*, Vol. 59, pp. 80–94.
- Müller-Wiener, W., 2007, *İstanbul'un Tarihsel Topografyası: 17. Yüzyıl Başlarına kadar Byzantion - Konstantinopolis – İstanbul*, Yapı Kredi Yayınları, İstanbul, Turkey.
- Ramos, L.F., L. Marques, P.B. Lourenc, G. Deroeck, A. Campos-Costa and J. Roque, 2010, “Monitoring Historical Masonry Structures with Operational Modal Analysis: Two Case studies” *Mechanical Systems and Signal Processing*, Vol. 24, pp. 1291–1305.
- Safak, E. and E. Çaktı, 2014, “Simple Techniques to Analyze Vibration Records from Buildings”, *7th European Workshop on Structural Health Monitoring*, La Cité, Nantes, France.

Toksoz, M.N. and A.A. Barka, 1989, "Seismic Gaps along the North Anatolian Fault", Abstract, *Proc. IASPEI Conference*, Istanbul, pp. 1-9.

Trifunac, M.D. and Brady, A.G., 1975, "A Study on The Duration of Strong Earthquake Ground Motion", *Bulletin of the Seismological Society of America*, Vol. 65, pp. 581-626.

Van Nice, R.L., 1963, "The Structure of St. Sophia", *Architectural Forum*, Vol. 118, pp. 45-138.